FACULDADE DE ENGENHARIA DE RECURSOS NATURAIS
ENGENHARIA BIOTECNOLÓGICA

Cranfield
UNIVERSITY

Silsoe
Cranfield Health
Master of Science in Molecular Medicine

Ana Rita Diogo Martins Vaz
Nº 20363

INVESTIGATION OF THE PRESENCE AND EXPRESSION OF THE CYCLOPHILIN A PSEUDOGENE IN NCI-H596 LUNG CELL LINE AND ITS EXPRESSION IN OTHER CELL LINES

Universidade do Algarve
Faculdade de Engenharia de Recursos Naturais
Engenharia Biotecnológica

&

Cranfield University
Cranfield Health
MSc in Molecular Medicine

Ana Rita Diogo Martins Vaz
N° 20363

INVESTIGATION OF THE PRESENCE AND EXPRESSION OF THE CYCLOPHILIN A PSEUDOGENE IN NCI-H596 LUNG CELL LINE AND ITS EXPRESSION IN OTHER CELL LINES

Supervisors: Dr Tracey Bailey
Dr José António Belo

August 2006

This thesis is submitted in partial fulfilment of the requirements for the degree of Master of Science

Abstract

Lung cancer is one of the most studied cancers and it is the number one cause of cancer deaths in Europe and United States. Prostate cancer is the most common malignancy among the males in the Western world and both of them are associated with several risk conditions.

Cyclophilin A pseudogene is a sequence present on the human chromosome 1 and when investigated by Inter-SSR PCR, showed an increase of intensity in the lung NCI-H596 cell line. After sequencing, a single nucleotide polymorphism was identified in that sequence.

In order to examine the relation between the single nucleotide polymorphism and cancer, the presence and expression of the PPIA pseudogene was studied in that lung cancer cell line and also in other cell lines from lung and prostate.

The cellular proliferation and morphology were also assessed showing that cancer cells and "normal" cells exhibited a certain number of differences. Cancer cells achieved higher levels of cellular proliferation compared with normal cells, probably due to the contact inhibition effect and anchorage dependent growth of normal cells. Morphologically, cancer cells did not exhibit constant characteristics compared to "normal" cell that grew as a uniform monolayer.

In order to test the viability of the genomic specific primers to anneal with the template DNA, three different annealing temperatures were tested during the optimization process of the PCR.

During the performance of the RT-PCR no results were obtained with the conditions that were applied to technique. It would be necessary perform further studies in order to know whether or not the PPIA pseudogene is being expressed in that particular lung cell line.

Acknowledgments

Firstly I would like to tank my mother and father for always supporting me in all my decisions and for giving me this great opportunity. Amo-vos muito.

Very special thanks to my uncle for always encourage me to go further.

Thanks to my very special friend Stephen who is always supporting me.

I would like to tank also Dr. Tracey Bailey who was my supervisor, Dr. Sarah Morgan and Jo for helping me in the lab, and Aurore, Ana, Natasha, Sarah, Namita and Emanuel for sharing some nice moments in the lab.

A very big thank you to Natasha, who helped me formatting my thesis.

Finally to all my friends that always gave me their incentive for being here.

Contents

List of Figures

List of Tables

Abbreviations

CDK – Cyclin Dependent Kinase

CGH – Comparative Genomic Hybridisation

DNA – Deoxyribonucleic acid

ECM – Extracellular Matrix

EGF – Epidermal Growth Factor

EGFR - Epidermal Growth Factor Receptor

GF – Growth Factors

Inter – SSR PCR – Inter-Simple Sequence Repeats Polymerase Chain Reaction

NSCLC – Non-Small Cell Lung Carcinoma

PCR – Polymerase Chain Reaction

PPIA – Peptidylpropyl Isomerase A

pRb – Retinoblastoma Protein

PSA – Prostate Specific antigen

Rb - Retinoblastoma

RNA – Ribonucleic Acid

RT-PCR – Reverse transcriptase - Polymerase Chain Reaction

SCLC – Small Cell Lung Carcinoma

WHO – World Health Organization

Chapter 1 – Introduction

1.1 – Cancer

Cancer is the result of uncontrolled duplication of abnormal cells, and presents an enormous public heath problem in the developed countries. Currently, it is the major cause of mortality in the UK and is diagnosed each year in one in every 250 men and one in every 300 women. In the United States one in four deaths is due to cancer. Usually, it is a costly disease to diagnose and investigate, and treatment is time consuming, labour intensive and normally requires hospital care. The most common cancers in the western world are the lung, breast, skin, gut and prostate [1], [2], [3].

This study will focus only on lung and prostate cancers.

1.1.1. Lung Cancer

1.1.1.a. Incidence

Lung cancer is one of the most studied cancers and it is the number one cause of cancer deaths in Europe and United States, and is a serious world health problem [4], [5].

The incidence of lung cancer is high in individuals around 65 years who started smoking before the age of 20 years old, allowing for the required induction time of the habit. However, after the age of 80 years the incidence declines because the habit of smoking between elder individuals is low and because people who reach such ages are thought to be genetically resistant to certain risk factors [4].

The disease kills nearly 160,000 people per year in North America, exceeding the deaths from colorectal, breast and prostate cancer combined. Until recently, lung cancer was the most frequently occurring cancer in the UK, however, it has been overtaken by breast cancer. It accounts for approximately 1 in 7 new cancer cases, corresponding to 37,700 new patients annually [4], [6], [7].

In terms of gender, there are more cases of lung cancer in men in Eastern Europe however the numbers of women being diagnosed has increased. In the other hand, in North America the incidence is higher in women [4], [5].

1.1.1.b Symptoms, Risk Factors, Classification and Diagnosis

The symptoms and signs of lung cancer are highly non-specific leading to a high lethality level. However the most common symptoms of this disease are cough most of the time, shortness of breath, coughing up phlegm (sputum) with signs of blood in it, ache or pain when breathing or coughing, loss of appetite, fatigue and lost of weight [4], [8].

There are several risk factors associated with this type of cancer. Some are intrinsic because they are inherent to the individual, such as genetic susceptibility, family history of cancer, sex, race, age and previous respiratory diseases, and others are extrinsic or environmental and are related with factors extraneous to the individual, such as tobacco use, diet, occupation and environmental pollution [4].

According to Barros-Dios et al (2003) the major causative factors in the development of lung cancer are the extrinsic ones, and the tobacco use is the main risk factor between them. It is estimated that approximately 85-90% of all pulmonary neoplasias derive from the habit of smoking [4].

Normal lung cells are transformed into cancer cells due to the carcinogenic substances contained into the cigarette smoke, and this risk of developing smoking-related lung cancer can be dependent on the duration and intensity of habit, age at initiation and type of tobacco [4], [6].

Occupation is also a strong extrinsic factor causative of lung cancer when workers are exposed to carcinogens in their place of work. In the European Union this scenario is real for 23% of the workers because they are engaged in occupations in which chemical compounds are handled or when their works involve the contact with dust or microscopic particles [4].

The family history is the major causative factor between the intrinsic risk factors and the second one after tobacco use. The risk is higher in individuals under the age of 59 years with a history of lung cancer among first-degree blood relatives. In the same way, first-degree blood relatives of any cancer sufferer have twice the probability of developing lung cancer, which is more common in families with a record of breast and ovarian cancer [4].

Lung cancer arises from transformed lung epithelial cells, progresses into a tumour mass which then may metastasize through lymph node channels and/or through direct invasion into blood vessels, and finally spread throughout the entire body [6].

The lung cancer diagnosis is based on several techniques such as chest x-ray which is the most common first diagnostic step when any new symptoms of lung cancer are present, computerized axial tomography scan that may be performed on the chest, abdomen, and/or brain to examine for both metastatic and primary tumour, Magnetic resonance imaging in order to indicate with precise detail about the location of the tumour, positron emission tomography used to determine whether a tumour tissue is actively growing and the type of cells within a particular tumour, several types of biopsy, etc.[9]

All biopsy samples are examined under a microscope by a pathologist in order to discover the origin of the cancer but if this procedure does not help further testing such as immunohistochemistry, electron microscopy, flow cytometry, cytogenetics and molecular genetic testing must be done [10].

The most widely accepted histologic classification for lung cancer tumours was proposed by the World Health Organization (WHO) in 1981, and the four major histologic types of lung cancer are squamous cell carcinoma, adenocarcinoma, small cell lung carcinoma (SCLC), and large lung carcinoma. These four different types of tumour can be subclassified into specific subtypes [11]. Squamous cell carcinoma, adenocarcinoma and large cell carcinoma are collectively referred to as non-small lung cancers (NSCLC) because their clinical behaviour and therapeutic approaches are similar [6].

1.1.2. Prostate Cancer

Prostate cancer is the most common malignancy in European males. In 2002 in Europe, an estimated 225,000 men were newly diagnosed with prostate cancer and about 83,000 died from this disease. In the United States of America between 2000 and 2005 more than 1 million men were newly diagnosed with this disease [12], [13].

Aging is the single most significant risk factor for prostate cancer however preneoplastic lesions named prostatic intraepithelial neoplasia can be found in men in their twenties and are fairly common in men by their fifties. Normally this disease

is not manifested until the age of 60 or 70 and the occurrence of precancerous lesions is significantly more prevalent (1 in 3 men) than the incidence of carcinoma (1 in 9 men) [14].

Prostate cancer is diagnosed by histological examination of prostate tissue which is obtained by ultrasound guided transrectal biopsy [12]. Currently there is no unequivocal serum or urine marker indicating the presence of prostate cancer, at least in its earlier stages [15]. Indications for biopsy are predominantly an aberrant digital rectal examination and/or an increased serum prostate specific antigen (PSA) which is not a prostate cancer marker [12], [13].

PSA is an enzyme synthesized by normal prostate cells and secreted in the prostatic fluid, a tiny amount of PSA is also released in the blood. Any acute or chronic, benign or malignant, prostatic disease will increase the "leak" into the bloodstream and increase the amount of detectable PSA [13]. The use of PSA testing has led to a lower tumour stage and grade at the time of diagnosis [12].

As in lung cancer, the stage of prostate cancer tells the doctor how far the cancer has spread and also provides the doctor with information about the best treatment to prescribe [16]. In its initial stages, when confined to the prostatic capsule, prostate carcinoma is essentially curable by surgical intervention and/or radiation therapy [14].

Prostate cancer arises from transformed prostate epithelial cells and progresses inside the prostate gland. It may then grow into the neck of the bladder or the seminal vesicle after breaking the covering of the prostate, and finally metastasize to another part of the body, most probably to the bones [16], [14].

1.2 – Cell Cycle and Alteration in Cancer

Like all eukaryotic cells, mammalian cells are bound to follow the cell cycle, during which DNA replication occurs followed by segregation of replicated chromosomes into two separated cells. The cell division is divided into two stages: mitosis (M), the process of nuclear division, and interphase which occurs between two M phases, as illustrated in figure 1.1 [17].

Mitosis includes four stages: prophase, metaphase, anaphase and telophase; and interphase includes three: G1, S and G2 phases. The replication of DNA occurs in phase S, then during phase G1, which precedes phase S, the cell is preparing for

DNA synthesis. Phase S is preceded by phase G2 where the cell prepares for mitosis [17].

Cells in G1 can, before commitment to DNA replication, enter a resting state called G0. In this stage, cells account for the major part of the non-growing, non-proliferating cells in the human body [17].

If the conditions are unsuitable for growth the cells may respond with cell death through a mechanism named apoptosis, the programmed cell death. All mammalian cells contain the genetic programme for apoptosis which results in the packaging of the whole cell into small membrane-bounded named apoptotic bodies. Conditions that provoke apoptosis include the lack of growth factors or serum, nutrient limitation and mechanical stress [18].

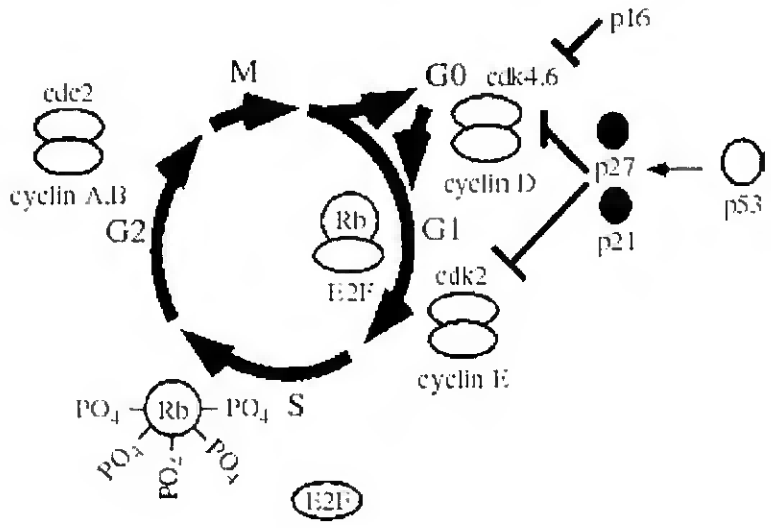

Figure 1.1 – The cell division cycle and its control [19].

In cancer, there are fundamental alterations in the genetic control of cell division, resulting in an unrestrained cell proliferation [17].

Mutations mainly occur in two classes of genes, the proto-oncogenes and the tumour suppressor genes. In normal cells, the products of proto-oncogenes act at different levels along the pathways that stimulate cell proliferation. Mutated versions of proto-oncogenes or oncogenes can promote tumour growth [17].

Inactivation of tumour suppressor genes like *p53* and *pRb* results in dysfunction of proteins which usually inhibit cell cycle progression. Cell cycle deregulation associated with cancer occurs through mutation of proteins important

at different levels of the cell cycle. In cancer, mutations have been observed in genes encoding CDK, cyclins, CDK-activating enzymes, CKI, CDK substrates, and checkpoint proteins [17].

1.2.1. The p53 tumour suppressor gene

The checkpoint or tumour-suppressor protein p53 is one of the important proteins encoded by checkpoint gene and mutations in that gene are present in over 50% of carcinomas of lung and bowel [19], [20]. It is a recessive gene and so a malignant transformation requires the functional loss of both copies of the gene, either two somatic mutational events or, in the presence of one mutated germline gene, with a single somatic mutation in its allele [20].

Both G1/S and G2/M check points are regulated by the p53 gene product however it does not appear to play an important role in the mitotic spindle check point since the gene knockout of p53 does not alter mitosis [19].

The p53 tumour-suppressor gene is the most frequently mutated gene in human cancer, indicating its important role in conservation of normal cell cycle progression. The amino-terminal sequences of p53 function as a transcriptional activation domain and the carboxy-terminal sequences appear to be required for p53 to form dimers and tetramers with itself [19].

It has been shown that the transcription of genes with roles in the control of the cell cycle, including WAF1/CIP1/p21 (encodes a regulator of Cdk activity), GADD45 (a growth arrest DNA damageinducible gene), MDM2 (encodes a protein that is a known negative regulator of p53), is activated by p53 [19].

One of the essential roles of p53 is to arrest cells in G1 phase after genotoxic damage, to allow for DNA repair prior to DNA replication and cell division. In response to massive DNA damage, p53 triggers the apoptotic cell death pathway. However tumour cells lacking normal p53 function do not arrest in G1 and are more likely to progress into S or G2/M and die [19].

The antiproliferative effect of the wild type p53 is mediated by stimulation of a 21 kDa protein (p21cip/waf1),a CKI, that inhibits cyclin-dependent kinase activity, including cyclin D/CDK4 or 6 as well as cyclin E/CDK2 and thereby cell division. So, the damaged DNA originates a signal that may activate p53 by post-translational modification. High p53 activity up-regulates p21CIP1, preventing the activation of

CDKs, required for the G1 to S transition. This negative cell cycle controller effect can be a reason to explain why the wild type p53 gene can suppress the transformation of cells by activated oncogenes, thus inhibiting the growth of malignant cells *in vitro* and suppressing the tumourigenic phenotype *in vivo* [19].

1.2.2. The pRb tumour suppressor gene

The pRb tumour suppressor gene is another fundamental cell cycle regulator and is located on chromosome 13q14, encoding the retinoblastoma protein (pRb). Gross DNA abnormalities in the Rb gene were found in approximately 20% of SCLC cell lines, while mRNA expression was absent 60% of cell lines [19].

Rb is a recessive gene and, in the same way as p53, malignant transformation requires loss of function of both copies on the gene. A germline mutation in hereditary retinoblastoma is characterized by early onset. In the other hand, loss of Rb function later in life is associated with SCLC and osteogenic sarcoma [20].

It is known that pRb is a master regulator for transcription. The presence of the Rb protein is essential for G1 to S phase transition in the cell cycle. This protein interacts with the E2F family of cell cycle transcription factors in order to repress gene transcription which is required for this transition, as illustrated in figure 1.1. pRb, through its interaction with E2F, also regulates genes that control apoptosis. The protein product of the retinoblastoma susceptibility gene is also able to form heteromeric complexes with cyclin D [19].

pRb not only regulates the activity of certain protein-encoding genes, but also the activity of RNA polymerase pol I and pol II transcription. It appears to be the most important factor in the regulatory circuit named restriction point which occurs in the late G1 phase [19].

The Rb pathway with 97 genes as physiological targets is a signal transduction pathway which is formed by the members of the Rb family. This pathway has an important role in cell cycle regulation and is involved in growth progression, differentiation and apoptosis in different organisms and cell types [19].

The checks and balances that exist between pRb and p53 involve the regulation of the G1/S transition and its checkpoints which are controlled by the E2F transcription family. It is also know that proliferation, cell death and differentiation of

distinct tissues are also intimately linked through entrance and exist from the cell cycle and thus through pRb and p53 pathways [19].

The cell is maintained by phosphorylation and dephosphorylation of the cell cycle gene products by cyclin/Cdk complexes, the last being a group of proteins present at the interphase cell [19].

1.2.3. Cyclins

Cyclins are a family of proteins which were firstly discovered in rapidly dividing cells and are implicated in the mitosis of all eukaryotes. They are 56 kDa proteins centrally involved in cell cycle regulation and they also are regulatory subunits of holoenzymecyclin through cell cycle checkpoints by phosphorylating and inactivating target substrates, as illustrated in figure 1.1 [19].

According to immunohistochemistry studies on hepatocellular carcinomas performed by Zhu M. H. et al. (2003), cyclins in different cell cycles were overexpressed at varied levels in that type of cancer. This may shorten the tumour cell cycle, accelerate cell proliferation, and have a close relationship with hepatocellular carcinomas aggressiveness [21].

Many hormones and growth factors that influence in turn cellular growth through signal transduction pathways, modify cyclin activity which, when de-regulated, provokes the acceleration of the cell cycle progression in transformed cells [19].

Cyclin A has some interesting roles among the cyclin family because it can activate two different cyclin-dependent kinases (Cdks) and function in both S phase and mitosis. Phosphorylation of components of the DNA replication machinery in S phase such as CDC6 by cyclin A-Cdk is believed to be important for initiation of DNA replication and to restrict the initiation to only once per cell cycle. In mitoses, the precise role of Cyclin A is not completely known, but it may play a role in the control of Cyclin B stability. During S phase cyclin A starts to accumulate and is destroyed before metaphase in advance of cyclin B which persists until metaphase. The overexpression of both cyclins A and E, especially the first one, was demonstrated by Li-Jian Liang (2003) in hepatocellular carcinomas lesions [19], [22].

Progression through each phase of cell cycle is controlled by the activity of different cyclin-dependent kinases (Cdks) and their regulatory subunits. The Cdks control the G1 to S phase transition whereas complexes such as Cdk2, cyclin E are

important for initiation of the S phase. Cdkcyclin complexes act on specific targets which belong to at least two major regulatory networks: the Rb-related/E2F pathway and complexes that are responsible for the initiation of DNA replication [19].

1.3 – Progression of Cancer

Progression of cancer is, in part, based on the multi-step process of carcinogenesis through progressive changes in both tumour suppressor genes and oncogenes which are responsible for the transformation of normal cells into malignant ones [6].

The multi-step process is caused by series of abnormalities which provoke the activation of distinct pathways named the "hallmarks of cancer" [6]. Hanahan et al. (2000) suggested that the cancer is a manifestation of six essential alterations, the hallmarks, in cell physiology that collectively lead to malignant growth, and which are self-sufficienty in growth signals, insensitivity to growth-inhibitory (antigrowth) signals, evasion of pro-grammed cell death (apoptosis), limitless replicative potential, sustained angiogenesis, and tissue invasion and metastasis [23].

Cancer cells have defects in regulatory circuits that govern normal cell proliferation and homeostasis. There are more than 100 distinct types of cancer, and subtypes of tumours can be found within specific organs [6].

In order to grow and metastasize hematogenically those tumours need to be supplied with oxygen and essential nutrients which happen through angiogenesis, the formation of new blood vessels [24].

The angiogenic factors are secreted when a growing tumour activates surrounding vessels provoking the "angiogenic switch" by changing the dormant tumour phenotype into an angiogenic one. Activated endothelial cells have to migrate toward the tumour along a newly formed matrix and the matrix components are synthesized by tumour cells and other cells such as macrophages and fibroblasts. The process of tumour angiogenesis is illustrated in figure 1.2 and can be divided into four stages:

Stage 1 – A small and dormant tumour can, depending on the nature of the tumour and its microenvironment, make the angiogenic switch to ensure exponential growth.

Stage 2 – The tumour secretes growth factors (GF) to activate endothelial cells of surrounding vessels.

Stage 3 – After activation, these endothelial cells start to migrate and proliferate toward the tumour. Only one endothelial cell starts an angiogenic sprout and develops into an endothelial tip cell migrating along the extracellular matrix (ECM) and guiding the following so-called stalk endothelial cells.

Stage 4 – Finally, the growing tumour is connected to the vasculature and later can metastasize [24].

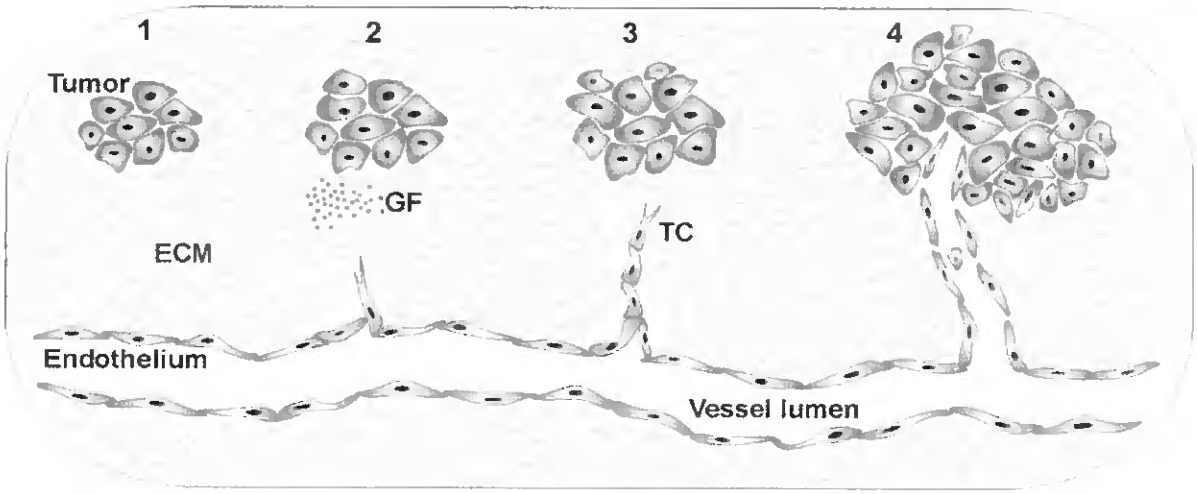

Figure 1.2 – The sequential steps during tumour angiogenesis [16].

After growth and proliferation, the tumour can metastasize. Malignant tumour cells, by invasion of the vessels, ECM degradation, attachment, and homing to target sites can form distal metastases [24].

The process of tumour angiogenesis results in a tumour-associated vasculature which is rather chaotic, both in structure and function. Tumour vessels have a non-continuous endothelium, an enlarged basal membrane, and an aberrant pericyte coverage, when compared with normal vessels [24].

1.4 – Genetic changes in lung cancer

Multiple genetic changes are involved in the development and progression of lung cancer, and have been identified as being inactivating mutations of tumour suppressor genes, activating mutations of oncogenes, amplifications of specific chromosomal regions and loss of heterozygosity which in other words means deletion of one of two copies of allelic DNA sequences in particular chromosomal regions. These molecular changes may be used as molecular markers for

differential diagnosis, assessment of the prognosis, and for lung cancer screening [25].

The genetic alterations leading to changes at the DNA level include point mutations, deletions, microsatellite instability and modifications of the promoter sites of the genes. Those changes in DNA lead to the cellular changes of RNA and protein levels which may originate an antibody response [25].

A large number of genetic changes have been identified in lung cancer however only few are described in the following sub-sections.

1.4.1. The p53 tumour suppressor gene

The p53 gene has an important role in lung cancer and mutations in this gene are most common in the evolutionarily conserved exons 5-8. There are several types of p53 mutations, including missense and nonsense mutations, splicing abnormalities as well as larger deletions [26].

One copy of the chromosomal region 17p13 which houses p53 is normally deleted in both SCLC and NSCLC, and mutational inactivation of the remaining allele occurs in 75-100% of SCLC and approximately in 50% of NSCLC. Most of the gene somatic mutations in p53 gene are missense and prolong the half-life of the p53 protein to several hours, increasing the protein levels which can be detected by immunohistochemistry. Immunohistochemical studies demonstrated that abnormal p53 expression in 40-70% of SCLC and 40-60% of NSCLC [26].

The majority of the p53 mutations in lung tumours are correlated with cigarette smoking. The most common p53 mutations in this organ are the G-T transversions which are expected from tobacco smoke carcinogens, such as benzo[a]pyrene. This carcinogen form adducts selectively along the p53 gene of bronchial epithelial cells, at the nucleotide positions [26].

1.4.2. The pRb tumour suppressor gene

RB mutations, together with loss of the wild-type allele, have been demonstrated in lung cancers. The RB protein is abnormal in more than 90% of SCLC and 15-30% of NSCLC. In lung cancers RB mutations include truncation by deletions, nonsense mutations, or splicing abnormalities and the majority of the

studies demonstrate that most of the mutations result in RB truncation. However, it is of great interest that a rare missense mutation in the RB `pocket' domain has been shown to cause defective RB phosphorylation and defective binding to oncoproteins [26].

The sensitivity for detecting RB abnormalities in SCLC varies methodologically: 20% by Southern blot analysis detecting band loss; approximately 60% by Northern blot analysis detecting absent or abnormal RNA; and approximately 90% by protein or immunohistochemical analysis. [26].

1.4.3. The $p16^{INK4}$ gene

The $p16^{INK4}$ gene is situated on chromosome 9p21 and frequently undergoes allele loss and mutation in a variety of human cancers including lung cancer. There were identified more than 120 point mutations and 50 other mutations including deletions, insertions, and splice mutations from a wide variety of cancers, indicating that there are several hot spots, some of which occur at conserved residues within the ankyrin domains of $p16^{INK4}$ [26].

The $p16^{INK4}$ protein is a cell cycle modulator which regulates the RB function by inhibiting CDK4:cyclin D1 kinase activity and is the third genetic target for mutations in the p16-cyclin D1-CDK4-RB pathway in lung cancer [26].

Homozygous deletion or point mutations in $p16^{INK4}$ have been observed in 10-40% of NSCLC. Those abnormalities are more often in NSCLC than SCLC [26].

$p16^{INK4}$ abnormalities are the most common mechanism for inactivating the p16-cyclin D1-CDK4-RB cell cycle control pathway in NSCLC, whereas RB inactivation is the preferential mechanism in SCLC. Thereby, lung cancers are characterized by either RB or $p16^{INK4}$ inactivation. Ten to thirty percent of NSCLC, appear to be normal for both RB and p16INK4, again stressing the likely contribution from abnormalities of cyclin D1, CDK4 and other members of this growth suppressor pathway. The majority, if not all, lung cancers have acquired genetic or epigenetic abnormalities in this p16/cyclinD1/CDK4/RB pathway [26].

1.4.4. Microsatellites

Microsatellite repeats are highly polymorphic, widely distributed throughout the genome and have been very useful markers for genetic mapping and analyzing small amounts of tumour samples for loss of heterozygosity [26].

Microsatellite instability, representing changes in the number of the short-tandem DNA repeats was initially reported in sporadic colorectal cancers and hereditary non-polyposis colon cancer where it reflects mutations of DNA mismatch repair genes, such as hMSH2, hMLH1, PMS1 and PMS2. Resulting in a distinctive `laddering' of short tandem repeat DNA sequences, such as dinucleotide repeats which are often called the replication error repair or RERá phenotype. Contrasting to the "laddering" of the RERá phenotype, a different and distinct "shift" of individual allelic bands which particularly affects tetra- or penta-nucleotide repeat markers, occurs in lung cancer. Thus, there appears to be only a single occurrence of unfaithful replication of an individual microsatellite marker which is then clonally preserved as the tumour develops [26].

Another difference from cancers such as colon and endometrial tumours, in which microsatellite instability usually affect multiple genetic loci concurrently, lung cancer frequently shows instability at only a few loci. These features together with the lack of reported mutations in the DNA mismatch repair genes in lung cancers have prompted suggestions that this is a distinct phenomenon and probably should be more accurately called "microsatellite alteration" (MA) or "genomic alteration" [26].

Overall, 35% of SCLC and 22% of NSCLC have shown some cases of MA at individual loci, but only 1-10% of all the samples show MA. Timing of genetic changes found in preneoplastic lesions of the respiratory epithelium accompanying primary NSLC [26].

1.5 – Genome analysis techniques

Genomic instability has been assessed by a wide range of techniques, such as comparative genomic hybridization (CGH), inter-simple sequence repeats polymerase chain reaction (inter-SSR PCR), chip-based CGH, flow cytometry,

arbitrarily primed polymerase chain reaction (PCR) and restriction landmark genome scanning, etc [27]. The first two techniques are mentioned below in more detail.

1.5.1. Comparative genomic hybridization

CGH is a molecular cytogenetic technique that provides an overview of changes in DNA copy number across the whole genome, analysing lesions of pure populations (90–100%) of morphologically defined cells from formalin-fixed, paraffin-embedded histological samples. However it is restricted to detecting nonreciprocal or unbalanced structural changes where there is a physical change in copy number of a region of the genome. Thereby, other structural rearrangements in the genome such as altered ploidy and balanced translocations cannot be identified through this method [27].

The methodology of CGH follows simple principles, but it is a labour-intensive and time-consuming method. The test (tumour sample) and reference (normal genomic sample) DNA are labelled with different fluorescent dyes, green and red respectively, and then mixed in a 1:1 ratio in the presence of human cot-1 DNA in order to block repetitive sequences, and finally co-hybridized to a representation of a genome, traditionally metaphase chromosomes prepared from cultured normal lymphocytes [28].

Specialized image analysis software coupled with a fluorescence microscope is used in order to capture the images of chromosomes and convert hybridization intensity data to a linear red–green ratio profile as illustrated in figure 1.3 [28].

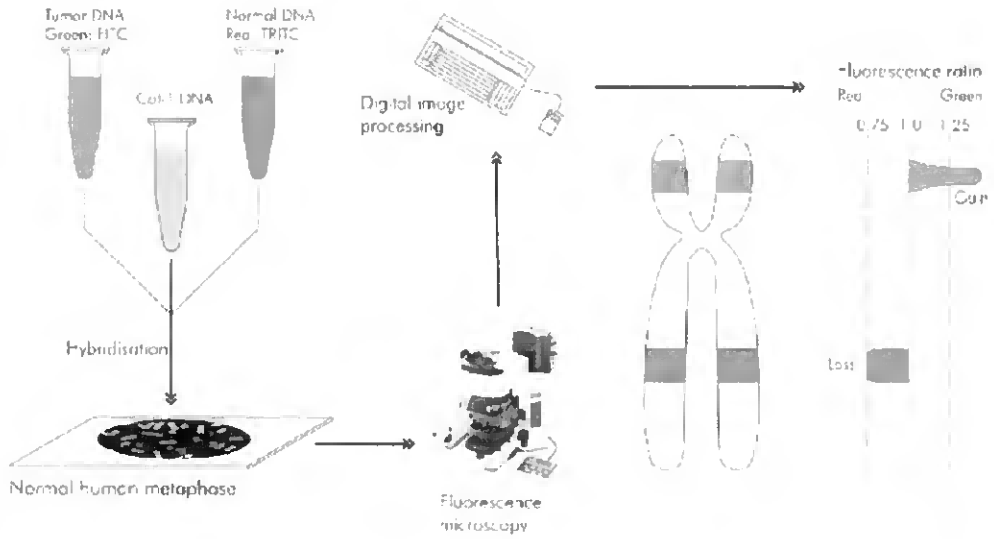

Figure 1.3 – Diagram illustrating the principles of comparative genomic hybridization (CGH). CGH: Tumour and reference DNA are labelled with green and red fluorophores, respectively, and hybridized to normal lymphocyte metaphase spreads. Fifteen–20 metaphases are captured using a fluorescence microscope coupled with a digital camera. Green to red signal ratios are quantified digitally for each chromosomal region along the chromosomal axis [28].

Deviations from a 1:1 ratio are counted as an important alteration in DNA copy number when defined thresholds are crossed and statistical verification applied. The purity of the cell population, and the extent and size of the alterations are limitations of this technique and which affect its sensitivity [28].

New chromosomal regions affected by either deletions or increased DNA copy number in lung cancer were identified by using the CGH methodology which has been applied to DNAs from cell lines as well as primary or metastatic lung cancers and has detected increased copy number consistent with amplification of underlying dominant oncogenes [26].

1.5.2. Inter-simple sequence repeats polymerase chain reaction

Inter-SSR PCR is a fingerprinting approach and has been proven to be a fast and reproducible methodology for quantification of deletions, insertions, and translocations in colorectal cancer. It has revealed a large number of changes and can be used to estimate the relative degree of genomic instability in tumours [27].

The methodology consists of the amplification of DNA segments between $(CA)_n$ dinucleotide repeats (microsatellites) using primers homologous to the repeats themselves but anchored at the 3' end by two nucleotides in order to prevent internal priming as illustrated in figure 1.4 [29].

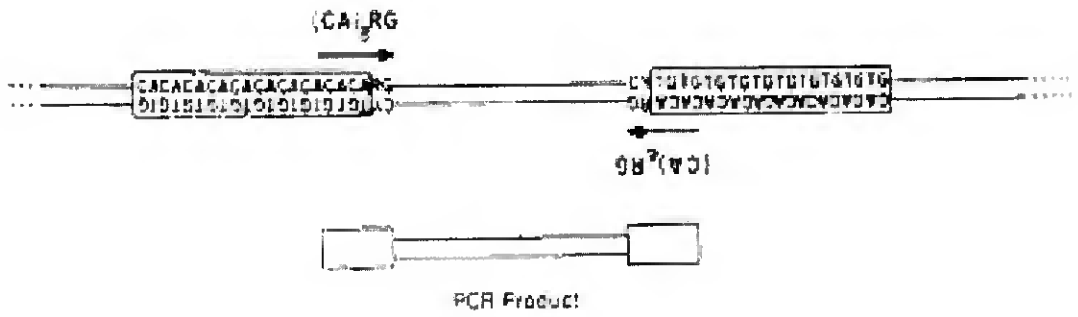

Figure 1.4 – Inter-simple sequence repeat (inter-SSR) PCR principle [21].

Closely adjacent repeat sequences arranged tail to tail are required for successful PCR amplification and since there are 50,000 to 100,000 $(CA)_n$ repeats in the human genome, such PCRs originates a high number of products which are resolved by polyacrylamide gel electrophoresis [29].

Specific alterations are detected as gains, losses, and intensity changes in electrophoretic bands and are likely to result from insertions, deletions, translocations, and amplifications, which are all genomic lesions believed to initiate with DNA strand breakage as illustrated in figure 1.5 [29].

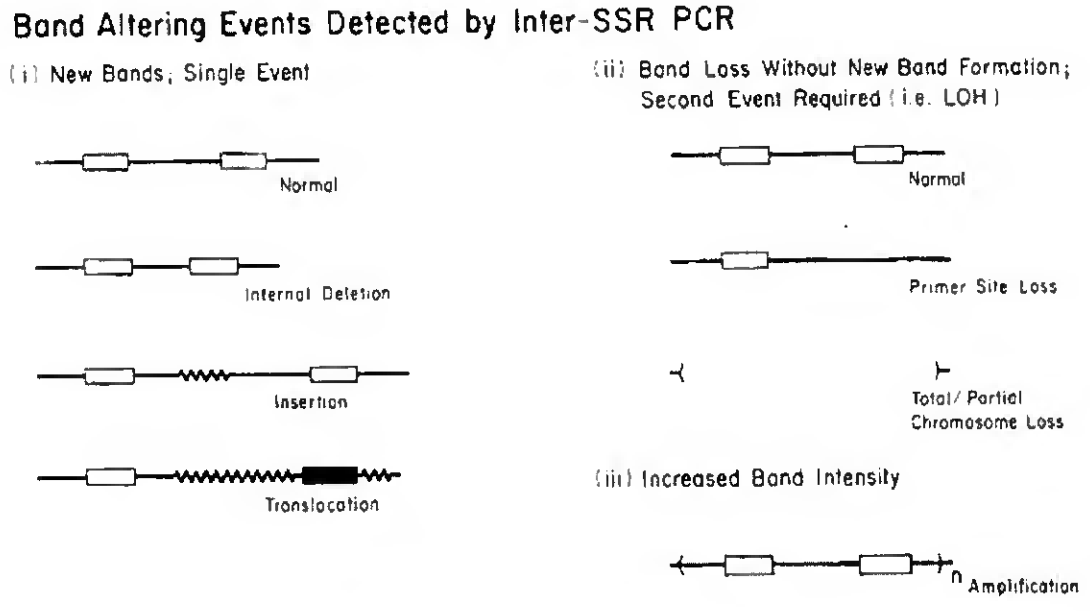

Figure 1.5 – Band altering events detected by Inter-SSR PCR [29].

These genomic alterations are not limited to insertions or deletions between or in the primer binding sites; larger scale processes such as deletions of portions of chromosomes or of entire chromosomes can also eliminate the corresponding bands [29].

This technique has four main advantages:

- Sequencing is not required to design the primers;
- Primers are anchored at the termini of the (CA)n repeats and extend into the flanking sequence by two nucleotide residues;
- Complex, species-specific patterns are obtained from a variety of eukaryotic taxa;
- Intraspecies polymorphism is observed, and it segregates as Mendelian markers [30].

David Broomhead (personal communication) Inter-SSR PCR to assess the occurrence and timing of DNA alterations in lung cancer progression via the *in vitro* model of carcinogenesis, studying the effect of a range of chemicals found within cigarettes by adding them to different lung cell lines [31].

Since this fingerprinting technique scans a vast range of the genome some of the Inter-SSR PCR products that were found by David Broomhead in his study code for proteins with a known or unknown function, or match non-coding regions of the genome. One of these products is the sequence of the peptidylprolyl isomerase A (cyclophilin A) (PPIA) pseudogene which showed an increase in intensity in the NCI-H596 cell line when compared to the other cell lines in study [31].

Cyclophilin A is an 18 KDa protein that belongs to the immunophilin family of proteins and with a wide variety of functions. Normally it is studied for thei binding of various immunosuppressive drugs, such as Cyclosporin A, and for its role in cellular signalling pathways. It also possesses peptidyl prolyl *cis*-trans isomerase activity and thus may have a role in protein folding. Campa et al. (2003) suggest that it can be involved in an important aspect of oncogenesis because of its role in cellular growth and differentiation, transcriptional control, cell signalling and immunosuppression [32], [33].

According to Burfeind et al. (2004), cyclophilin A was found to be overexpressed in prostate carcinoma and in lung cancer, and highly expressed in human breast ductal carcinoma and in hepatocellular carcinoma [34].

1.5.3. Techniques Required to Identify Genome Changes

Inter-SSR PCR is a technique able to demonstrate that a genomic alteration has occurred, however it is still necessary to identify that alteration. This last step can be done by cloning and sequencing of the altered bands from the polyacrylamide gel [27], and finally by using the bioinformatics tools such as the BLAST search on the National Centre for Biotechnology Information (NCBI) website, to search for homology with other sequences in the human genome [31].

In order to accomplish the sequencing of the altered DNA bands, the corresponding bands are subjected to re-electrophoresis on a nondenaturing polyacrylamide gel. Then the DNA is extracted by boiling, and the products are re-amplified by PCR and cloned into a plasmid vector [27].

According to Broomhead, the recovered inter-SSR PCR sequence of 491 bp, shown in figure 1.6, was inserted into the BLAST search engine and the NCBI database was searched, supplying with precise identification of the abnormal band and as well with additional information about its chromosomal location and homology [31].

```
56461 atgcaatcac acacacacac acacacacac aatcacacac gggcaccttg caaattgctc
56521 tccccacccc tcttctggaa actacaattt taccctcata caagtccgca gtcccttatc
56581 taaaactctt ggggtcagat acatttcaga cttcagaatg tgtctgattt tagaagggga
56641 atttggtgca tataccatag atttcataat aacctctgta gggcctgagc agcactcagt
56701 aagcaaacgt gactatttct gcagtgaaat gtgtgaatat tcacagtaag tgggggaaaa
56761 taaaggccat aaatagcctc atgacatttc aagttgtgtt ttaccagact tatgagttaa
56821 tagaaaacac ggcctttgga gcttcttgga tttcaggatc gcaggtgagt gcctctcacg
56881 agtccctcag ccaggtgggc tgctcagccc tgatgtacac caacccacat atttgttcac
56941 ttgtaataaa tgtcaagagc catattcttg ccatgggagc agaagggacg gggctgtgtg
57001 tgtgcgtgcg tgtgcgtgtg cgtgtgcatg cgcacctaca tacacgtcca cataccagga
```

Figure 1.6 – Part of the cyclophilin A pseudogene sequence where the genomic alteration was identified. Where is a thymine (t) in red should be a cytosine (c).

The sequence was found to have 98% of homology to a human DNA sequence from clone RP11-415K20 on chromosome 1 which is thought to contain a cyclophilin A pseudogene. There was a single base change between the test sequence and the altered base sequence. The normal sequence has a thymine (t) in that position but the mutated one has a cytosine (c), as illustrated in red in figure 1.6. There is no literature available mentioning this pseudogene and its possible relation with cancer or with other human biological systems [31].

1.6 – Pseudogenes

Originally, pseudogenes were defined by their possession of sequences that are related to those of the functional genes, but were thought not to be translated into a functional protein [35].

Some pseudogenes present the same general structure as functional genes, with sequences corresponding to exons and introns in the usual locations. They may have been turned inactive by mutations which prevent any or all of the stages of expression. The changes can provoke the elimination of the signals for initiating transcription, can avoid splicing at the exon-intron junctions, or prematurely terminating translation [35].

Usually a pseudogene has several deleterious mutations. Once it was stopped being active active, there is no impediment to the accumulation of further mutations. Pseudogenes that represent inactive versions of currently active genes have been found in many systems, including globin, immunoglobulins, and histocompatibility antigens, where they are located in the vicinity of the gene cluster, often interspersed with the active genes [35].

Processed pseudogenes may arise from reverse-transcription of mRNA and re-integration into the genome. They are probably made as a by-product of LINE retrotransposition. In other words, the processed pseudogene is formed from reverse transcribing a spliced mRNA into a cDNA using the reverse transcriptase from the LINE and re-integrating into the genome [36].

Duplicated pseudogenes tend to arise for organism-specific environmental response functions which may reflect genomic mechanisms that an organism uses to generate proteins that deal with alterations in its environment. Gerstein et al (2002) suggest that pseudogenes or pseudogenic parts for such classes of gene may occasionally be resurrected and used to enable larger random leaps in sequence space [36].

Non-functional as well functional transcripts of pseudogenes have been described in many organisms. There are numerous human examples which include the interferon pseudogene, glucocerebrosidase pseudogene, dopamine D5 pseudogene, DNA topoisomerase 1 pseudogene, ect [37].

According to Broomhead (personal communication), the cyclophilin A pseudogene showed an increase in intensity in the NCI-H596 cell line when

compared, by Inter-SSR PCR, to the other cell lines in study [23]. This fact might suggest that this pseudogene expression is possible.

Pseudogenes might have a possible function in development as a source of intracellular inhibitors. Once there is a possibility of pseudogenes being the source of the antisense RNA by that hybridizes with the sense RNA from the determinator genes and blocking their expression. They may be transcribed from the opposite strand relative to their functional counterparts, making them a source of antisense RNA [36].

1.7 – Objectives

The main aim of this study was to investigate the presence and expression of the cyclophilin A (PPIA) pseudogene sequence which was thought to be altered in a particular lung cancer cell line (NCI-H596) and its expression in other cell lines.

1.7.1. Cell Culture

In an *in vitro* cell model, like the one that was used during this study, it is necessary to recreate and control all the physico-chemical parameters in order to give to the cells the same environment that they would have in the body. Such parameters include the pH, temperature, osmotic pressure, levels of oxygen and carbon dioxide, and culture media supplements.

The culture media required for the propagation of animal cells are much more complex than the minimal media sufficient to support the growth of bacteria and yeasts. In addition to salts and glucose, the media used for animal cell cultures contain various amino acids and vitamins, which the cells cannot make for them selves. The growth media for most animal cells in culture also include serum, the major cost component, which serves as a source of polypeptide growth factors which are required to stimulate cell division [38].

By using those conditions and basic cell culture techniques the lung and prostate cell lines are grown in order to extract the DNA and total RNA which are then used to perform the polymerase chain reaction (PCR) and reverse transcriptase (RT) reactions in order to investigate whether or not the PPIA pseudogene is being expressed.

1.7.2. Reverse Transcriptase – Polymerase Chain Reaction

Analysis of gene expression requires accurate determination of the mRNA levels. However polymerase chain reaction (PCR) is based on amplification of DNA rather than RNA, so the solution is convert the mRNA into DNA using the reverse transcription process [39].

Reverse transcriptase – polymerase chain reaction (RT-PCR) is based on the capacity of the enzyme reverse transcriptase to generate a complementary strand of DNA (first-strand cDNA) using the mRNA as a template. This complementary strand is then amplified by PCR reaction by using forward and reverse primers which are specific to the target gene [39].

Finally the results are revealed by running the PCR products into an agarose gel.

By using this technique during this study should be possible to see whether or not the cyclophilin A pseudogene is being expressed or not. If it is being expressed, is then necessary find out if it is happening only in lung adenosquamous carcinoma cell line (NCI-H596) or also in the others cell lines.

Chapter 2 – Materials and Methods

2.1 – Cell growth *in vitro*

2.1.1. Cell lines and media requirements

The four cell lines cultured during the project are originated from human lung and prostate.

Lung adenosquamos carcinoma (NCI-H596) is the cell line in which the possible overexpression of the PPIA pseudogene is being investigated. This cell line is derived from a tumour mass in the chest wall of a 73-year-old male Caucasian patient with adenosquamous carcinoma (NSCLC) of the lung. It is a near triploid human cell line possessing a modal number of 71 chromosomes, expressing easily detectable levels of p53 mRNA whilst not exhibiting gross structural DNA abnormalities [40].

The others cell lines being investigated are "normal" lung (HBE 135-E6E7), prostate adenocarcinoma (PC-3) and "normal" prostate (PNT-1A). The HBE135-E6E7 cell line was established from normal bronchus tissue taken at lobectomy for squamous cell carcinoma from a 54-year-old male. The cells from the primary explant in their first passage were infected and immortalized with the recombinant retrovirus LXSN16E6E7 containing the human papilloma virus (HPV) E6E7 gene. This cell line express high levels of mRNA for epidermal growth factor receptor (EGFR), transforming growth factor-alpha (TGF-alpha), and amphiregulin (AR), however do not express epidermal growth factor (EGF) which has to be supplied with the growing media [41].

The PC-3 cell line was initiated from a bone metastasis of a grade IV prostatic adenocarcinoma from a 62-year-old male Caucasian. It is a near triploid cell line with a modal number of 62 chromosomes, exhibiting low acid phosphatase and testosterone-5-alpha reductase activities [42].

The PNT-1A cell line was established by immortalisation of normal adult prostatic epithelial cells by transfection with a plasmid containing SV40 genome with a defective replication origin. The primary culture was obtained from the prostate of a 35-year-old male at post mortem and the cells express cytokeratin 8 and 18, and vimentin [43].

The media requirements are different for different cell lines. The NCI-H596, PNT-1A cell lines grew in 500 ml RPMI-1640 media supplied with 10% (v/v) foetal calf serum (FCS), 1 ml penicillin/streptomycin solution, 1 ml amphotericin and 4 ml L-glutamine (media and supplements all from Invitrogen, Paisley, UK).

The HBE135-E6E7 cell line grew in 500ml Keratinocyte-Serum Free (KSF) (Invitrogen, Paisley, UK) media supplied with 5 mg (ng/ml) human recombinant EGF (Invitrogen, Paisley, UK), 0.05 mg/ml bovine pituitary extract (BPE) (Invitrogen, Paisley, UK), 0.005 mg/ml insulin (Sigma, Steinheim, Germany) and 500 mg (ng/ml) hydrocortisone (Sigma, Steinheim, Germany).

The PC-3 cell line grew in 500 ml RPMI-1640 media supplied with 10% (v/v) foetal calf serum (FCS), 1 ml penicillin/streptomycin solution, 1 ml amphotericin and 2 ml L-glutamine (media and supplements all from Invitrogen, Paisley, UK).

2.1.2. Cell culture techniques

2.1.2.a Thawing the cells

The vials were removed from bank to be thawed and silver foil was placed over the lid of the vials. One at a time was held in the water bath (Grant, Cambridge, UK) at 37°C until the last crystal was thawed.

Each vial was then sprayed with 70% isopropanol (v/v) (Fisher Scientific, Loughborough, UK) and placed in the cell culture hood (Haraeus, Germany). Its contents were removed and placed in 15ml centrifuge tube (Fisher Scientific, Loughborough, UK). One drop of appropriate cell culture media was added using a plastic Pasteur pipette (Fisher Scientific, Loughborough, UK), then swirled, another added drop and swirled again. This was repeated until the total volume was 5 ml taking approximately 5 min. Over the next minute a further 5 ml of media were added with gentle swirling.

The tube was centrifuged (Jouan, Winchester, USA) at 1300 rpm (100g) for 5 min at 4°C, then the supernatant was removed and the pellet was resuspended in 1ml of media. The suspension was placed into a T25 flask (Nunc, Rosklide, Denmark) and supplemented with a further 6ml of media. To ensure equal distribution of cells the flask was swirled gently and then placed in the incubator (Sanyo, Japan) at 37°C. The flask was checked next day under the microscope and the media was replaced.

When 75-80% of confluence was achieved, the cells were placed into a T75 flask (Nunc, Rosklide, Denmark) using the splitting procedure (See section 2.1.2.c).

2.1.2.b Feeding the cells

Once the cultures were established they were checked daily and the media replaced every 2 days. Normal cultures present a light pink, turning yellow colour. The media should always be clear. The appearance of turbidity means either the culture has become infected or the cells have detached.

The fresh media was warmed to 37°C and the waste beaker was prepared as explained in appendix A. The flasks were removed from the incubator (Sanyo, Japan) with only one cell line in the hood at a time. Then the media was removed and replaced from one flask at a time taking care to not touch the neck of flask.

2.1.2.c Splitting the cells

When the cells reached 75-80 % confluence in the flask, they were split. The simplest way to do this is to use trypsin/EDTA to detach the cells.

Trypsin/EDTA (10x) (Invitrogen, Paisley, UK) was thawed, sterile PBS and media were warmed to 37 °C and then placed into the hood. 1x trypsin/EDTA was done by adding 9ml PBS (Invitrogen, Paisley, UK) to 1ml trypsin concentrate.

The media was removed from the flask and the residual media was rinsed away using sterile PBS. After this, 5 ml 1x trypsin solution was added and the flask was placed in the incubator for not longer than 5 min and then checked under the microscope to see if cells were detached.

Approximately 5ml of media was placed in a 15ml centrifuge tube (Fisher Scientific, Loughborough, UK) and the cell suspension was added to neutralise the trypsin activity. The tube was then centrifuged at 1300 rpm (100g) for 5 min at 4°C, and the pellet resuspended in 5 ml media for plating.

Finally 1ml cell suspension was added to a clean sterile T75 flask (Fisher Scientific, Loughborough, UK) followed by 9 ml media. The flask was gently swirled to ensure adequate dispersion of cells and then placed in the incubator (Sanyo, Japan).

2.1.2.d Cell counting

The cell counting was accomplished in order to perform the growth curves of the different cell lines, and see if they had any inherent differences in growth characteristics. The cells were trypsinised using the same procedure as to split cells (see section 2.1.2.c). Then the pellet was re-suspended in 2 ml PBS and 100µl were transferred to a 0.5ml tube. 100µl trypan blue (Sigma, Steinheim, Germany) was added and these solutions were then mixed together giving a final volume of 200µl and left to stand for 1 minute. While the mixture was resting, the Neubauer haemocytometer (Assistant, Germany) was prepared as illustrated in figure 2.1.

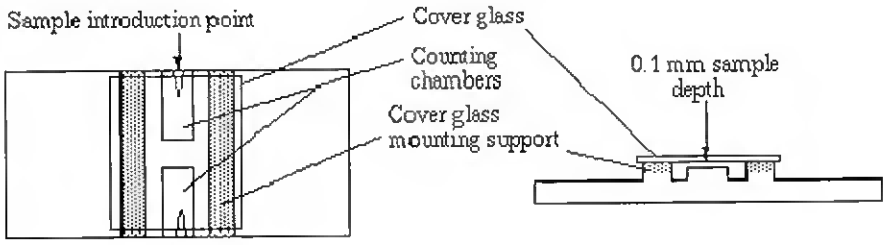

Figure 2.1 – A cover slip is moistened with a solution containing a mixture of the re-suspended pellet in PBS and trypan blue, and then placed on the haemocytometer covering the 2 central channels [44].

Approximately 20µl of the mixture was dispensed underneath the cover slip at the sample introduction point until the whole counting chamber was filled by capillary action.

The cell count was then performed according to the following rules: the haemocytometer contains 2 identical grids, one on the upper counting chamber and one on the lower counting chamber as illustrated in figure 2.2. Each counting grid consists of four corner squares containing 16 smaller squares and one central square containing 25 squares. When viewed under a microscope, if the cell number exceeded 200 when counting the central square alone, then only the 2 central squares on both grids were counted and an average was calculated. However if the cellular number does not exceeded 200, then all 4 corner squares were counted on each counting grid plus the central square and an average was calculated.

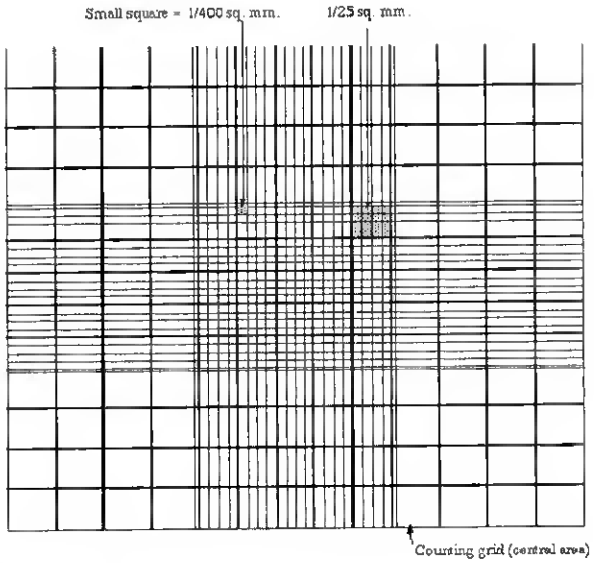

Figure 2.2 – Diagram of the grid on the haemocytometer each of the 9 squares is 1mm and the depth between the coverslip and grid is 0.1mm [44].

For cells that overlap a grid line, count a cell as "in" if it overlaps the top or right ruling, and "out" if it overlaps the bottom or left ruling. Once the cellular average was calculated the total number of cells in the 2ml suspension was also calculated:

Total number of cells = Average × 10000[a] × 2 (dilution factor)

[a]Conversion factor 1mm to 1ml 0.1µl = 1mm

Finally the number of cells per ml was calculated simply by dividing by 2.

2.1.2.e Scraping the cells

The media was removed from the flask and the residual media was rinsed away using sterile PBS (Invitrogen, Paisley, UK). Then 10 ml PBS were added and, using a scraper (Nunc, Rosklide, Denmark), the cells were detached from the flask surface.

The resulting suspension was transferred to a 15 ml centrifuge tube (Fisher Scientific, Loughborough, UK) which was placed into the centrifuge at 3000 rpm (230g) for 10 min at 4 °C. The supernatant was removed and 1 ml PBS was then added to the pellet and resuspended.

This new suspension was transferred to a 2 ml gamma irradiated tube (Fisher Scientific, Loughborough, UK) and centrifuged (ALC, Italy) at 11500 rpm for 15 min. The supernatant was removed and the cells were frozen with liquid nitrogen and finally the tubes were placed into the freezer (Revco).

2.2 – Nucleic acids extraction

The nucleic acids, DNA and total RNA, were extracted from the pelleted cells using Qiagen extraction kits in order to test the viability of the primers and study the mRNA expression of the PPIA pseudogene, respectively. To extract DNA, the QIAamp® DNA mini kit (Qiagen, Crawley, UK) was used and to extract the total RNA the RNeasy® Mini Kit (Qiagen, Crawley, UK) was used. Those kits were used because they ensure a fast and easy extraction and a final product with high purity and good yields.

2.2.1. Extraction of DNA

The frozen cell pellet was re-suspended in 200μl of PBS (Invitrogen, Paisley, UK) and transferred to a 1.5 ml microcentrifuge tube (Fisher Scientific, Loughborough, UK) and then 20μl QIAGEN Proteinase K (Qiagen, Crawley, UK) were added, followed by 200μl buffer AL (supplied in the kit). The mixture was mixed by pulse-vortexing (Hook & Tucker, Croydon, England) for 15 seconds and incubated at 56°C for 10 minutes in a water bath (Grant, Cambridge, UK).

Then, the mixture was briefly centrifuged (Beckman, Germany) to remove drops from the inside of the lid and 200μl ethanol (96-100% v/v) (Fisher Scientific, Loughborough, UK) was added. The mixture was mixed again by pulse-vortexing (Hook & Tucker, Croydon, England) for 15 seconds and then briefly centrifuged to remove drops from the lid.

Carefully the mixture was applied into the QIAamp Spin Column (in a 2ml collection tube supplied in the kit) without wetting the rim. The cap was closed and the mixture was centrifuged at 8000 rpm (6000g) for 1 minute. Then the QIAamp Spin Column was placed in a clean 2ml collection tube and the tube containing the filtrate was discarded.

The QIAamp Spin Column was opened carefully and 500µl buffer AW1 (supplied in the kit) was added without wetting the rim. The cap was closed and the mixture was centrifuged again at 8000 rpm (6000g) for 1 minute. Then the QIAamp Spin Column was placed in a clean 2ml collection tube (supplied in the kit) and the tube containing the filtrate was discarded.

Carefully the QIAamp Spin Column was opened and 500µl buffer AW2 (supplied in the kit) was added without wetting the rim. The cap was closed and the mixture was centrifuged at full speed (14000 rpm; 20,000 g) for 3 minutes.

The QIAamp Spin Column was placed in a clean 1.5ml microcentrifuge tube and the tube containing the filtrate was discarded. Carefully the QIAamp Spin Column was opened and 200µl buffer AE (supplied in the kit) was added. The mixture was incubated at room temperature (15-25°C) for 1 minute, and then centrifuged at 8000 rpm (6000g) for 1 minute. The resulting filtrate contained the extracted DNA.

Finally, the DNA was quantified (See section 2.2.3.a).

2.2.2. Extraction of total RNA

The tube was flicked after the cells were thawed and, to disrupt the cells, 600 µl RLT buffer (supplied in the kit) (Qiagen, Crawley, UK) was added to the pellet. Then the vortex (Hook & Tucker, Croydon, England) was used to mix.

To homogenize the sample, the lysate was passed at least 5 times through a 20-gauge needle (0.9 mm diameter) fitted to an RNase-free syringe (BD Discardit™II, Huesca, Spain).

600 µl 70% (v/v) ethanol (Fisher Scientific, Loughborough, UK) was added to the homogenized lysate, and the sample was mixed well by pipetting and applied (600 µl at a time) to an RNeasy® mini column placed in a 2 ml collection tube (supplied in the kit). The tube was gently closed and the mixture was centrifuged for 1 min at 10,000 rpm (8000g). The flowthrough was discarded and the collection tube reused.

700 µl of Buffer RW1 (350 µl at a time) was added to the RNeasy® column. The tube was gently closed, and the sample was centrifuged for1 min at 10000 rpm (8000g) to wash the column. The flow-through and collection tube were discarded.

The RNeasy® column was transferred into a new 2 ml collection tube and 500 µl of buffer RPE (supplied in the kit) was added onto the RNeasy® column. The tube was gently closed and the sample was centrifuged for 1 min at 10000 rpm (8000g) to wash the column. The flow-through was discarded and the collection tube reused.

Another 500 µl Buffer RPE (supplied in the kit) was added to the RNeasy column. The tube was closed gently, and the sample was centrifuged for 2 min at 10000 rpm (8000g) to dry the RNeasy® silica-gel membrane.

To elute the RNA, the RNeasy® column was transferred to a new 1.5 ml collection tube and then 50µl RNase-free water was added directly onto the RNeasy® silica-gel membrane. The tube was gently closed, and the sample was centrifuged for 1 min at 10000 rpm (8000g) to elute.

Finally, the total RNA was quantified (See section 2.2.3.b).

2.2.3. Nucleic acids quantification

2.2.3.a DNA quantification

The quantity and purity of the DNA were determined by diluting the DNA sample 1 in 25 in distilled water in a quartz cuvette (Sigma, Steinheim, Germany) and measuring the absorbance at 260 and 280nm against distilled water.

The quantity of DNA was determined through the following formula:

$$\mathbf{Q_{DNA} = A_{260} \times DF \times 50}$$

Where:

Q_{DNA} – Quantity of DNA (ng/µl),

A_{260} – Absorbance of the sample at 260 nm,

DF – Dilution Factor which is 25,

50 – Quantity (ng/µl) of double stranded DNA corresponding to 1 unit of absorbance at 260nm.

The purity of DNA was determined through the following ratio:

$$\text{Purity} = A260 / A280$$

A value between 1.7 – 1.9 was considered to be pure.

2.2.3.b Total RNA quantification

The quantity and purity of the total RNA were determined by diluting the DNA sample 1 in 100 in distilled water in a quartz cuvette and measuring the absorbance at 260 and 280nm against distilled water.

The quantity of total RNA was determined through the following formula:

$$\mathbf{Q_{total\ RNA} = A_{260} \times DF \times 40}$$

Where:

$\mathbf{Q_{total\ RNA}}$ – Quantity of RNA (ng/µl),

$\mathbf{A_{260}}$ – Absorbance of the sample at 260 nm,

DF – Dilution Factor which is 100,

40 – Quantity (ng/µl) of RNA corresponding to 1 unit of absorbance at 260nm.

The purity of RNA was determined through the following ratio:

$$\text{Purity} = A260 / A280$$

A value equal to 2 was considered to be pure.

2.3 – Nucleic acids amplification

2.3.1. Reverse transcriptase (RT)

The total RNA samples previously obtained were placed on ice to thaw along with the Cloned AMV First-Strand cDNA Synthesis Kit (Invitrogen, Paisley, UK).

Firstly 4µl of the total RNA was added to a 0.5ml RNase free PCR tube. Then 2µl of 10mM dNTP Mix (supplied with the kit) and 1µl (50ng/µl) random-hexamer or Oligo$(dT)_{20}$ primers (supplied with the kit) or 10µM gene specific primer were added. This solution was then incubated for 5 minutes at 65˚C (Grant, Cambridge, UK) to denature the RNA and primer and then incubated again for 2 further minutes at room temperature.

During the incubation period, the following master mix was prepared for each reaction. Into a RNase free tube, 4µl of 5 x cDNA synthesis buffer was added followed by, 1µl 0.1M DTT, 1µl RnaseOut™ (40 units/µl), 1µl DEPC-treated water and 1µl of cloned AMV RT (15 units/µl) (all master mix components supplied with the kit). This solution was then mixed by vortexing (Hook & Tucker, Croydon, England) and 8µl of this master mix was added to each reaction tube at room temperature. The samples were then placed into the thermal cycler (Techne, Cambridge, UK) at 50˚C for one hour and then at 85˚C for 5 minutes. The cDNA could then be used immediately or stored until required at -20˚C (Hotpoint, UK).

2.3.2. Polymerase chain reaction (PCR)

The PCR was performed using the Qiagen Taq PCR Core kit (Qiagen, Crawley, UK), in a 20 µl reaction final volume, containing 1x PCR buffer already supplied with 1.5 mM of $MgCl_2$; 0.4 nM of dNTPs; 1µM (20 pmol) of both reverse and forward primers which are showed in table 2.1,; 0.6 µl (1 unit working) of Taq DNA polymerase; 6 µl of distilled water and finally 1 µl of template DNA solution.

Table 2.1– DNA sequences of the forward and reverse primers used to accomplish the PCR reaction designed by David Broomhead [31].

Primer	Sequence
Forward	CTC TCC CCA CCC CTC TTC TG
Reverse	AGC CCC GTC CCT TCT GC

After the mixture was dispensed into the PCR tubes, these were placed inside the thermal cycler (Techne, Cambridge, UK) and the program with the following conditions was performed:

Initial Denaturation	3 minutes	94 °C
35 cycles:		
Denaturation	30 seconds	94 °C
Annealing	45 seconds	52 / 58 / 55 °C
Extension	2 minutes	72 °C
Final Extension	7 minutes	72 °C
Final hold	Held at	4 °C

Three different annealing temperatures were tested during the study: 52, 58 and finally 55°C.

A positive control performed with the β-actin primers, figure 2.2, and a negative (no template) controls were also included to validate the amplification reactions.

Table 2.2– DNA sequences of the β-actin forward and reverse primers used to perform the positive control during the RT-PCR and which were designed by Ryan Pink.

Primer	Sequence
Forward	CTA GAA GCA TTT GC
Reverse	TGA CGG GGT CAC TCT GC

2.3.3. Electrophoresis

PCR products were analysed by agarose gel electrophoresis. A 2% (w/v) agarose gel in tris-acetate-EDTA (TAE) buffer was prepared (see appendix A). The gel was placed into the submarine equipment (Embitec, San Diego, USA) (making sure the orientation of the gel was correct with respect to the electrodes – running negative to positive) and the tank filled with TAE buffer, covering the gel surface.

Then 10 of PCR samples was diluted with 2 µl loading buffer (Promega, Madison, USA) and a final volume of 8µl loaded into the separate wells. 4 µl 100bp DNA ladder (Promega, Madison, USA) was loaded alongside. The lid was

connected and electrophoresis performed at 100V for about 30 minutes. On completion, the voltage was turned to zero, the power supply was switched off and then the mains. The gel was removed and placed in a 0.5µg/ml solution of ethidium bromide (Sigma, Steinheim, Germany) for 10-30 minutes. The staining pattern was observed under UV light in a bioimaging system (Genius).

Chapter 3 – Results

3.1 – Cellular proliferation

Cellular proliferation is the result of cell growth and division which increase the number of cells in culture. Considering the cellular proliferation growth curves, it was possible to compare the cellular growth between cancer and "normal" cells.

3.1.1. Lung cell lines

3.1.1.a HBE 135-E6E7 cell line

The T25 flasks were seeded with approximately $9x10^4$cells/ml and the growing rate was monitored. Lag phase had a duration of 48 hours, as illustrated in figure 3.2. The peak of the exponential phase was reached after 144 hours of growth and the number of cells was approximately $3.5x10^5$/ml. The stationary phase was almost non-existent and the number of cells began to decrease immediately after the exponential phase.

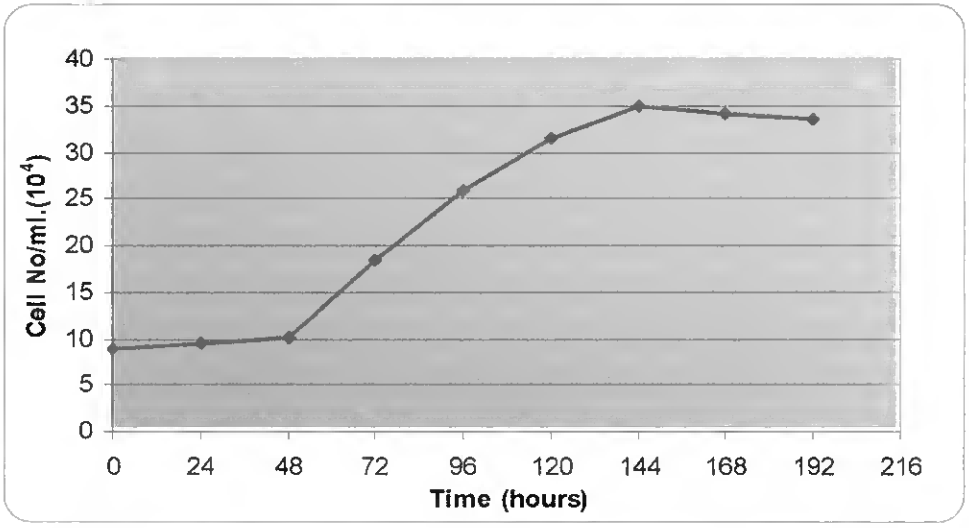

Figure 3.1 – Cellular proliferation of the HBE135-E6E7 ("normal" lung) cell line.

3.1.1.b NCI-H596 cell line

The T25 flasks were seeded with approximately $9x10^4$cells/ml and the growing rate was monitored. As illustrated in figure 3.1, the adaptation or lag phase, during which the number of cells remains relatively constant after the exponential phase, had a duration of 48 hours. The peak of the exponential phase was reached after 144 hours of growth when the number of cells was approximately $4.6x10^5$/ml. This phase was followed by a stationary period of almost 48 hours and then the number of cells started decreasing.

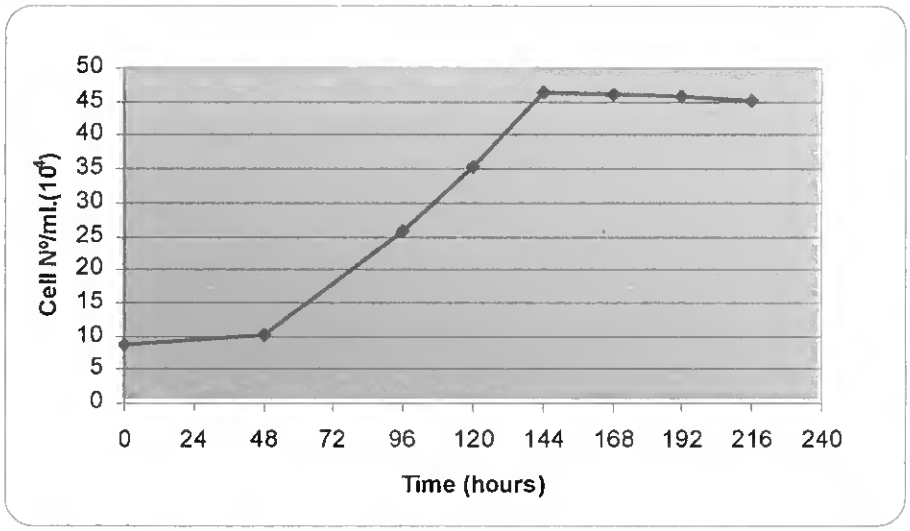

Figure 3.2 - Cellular proliferation of the NCI-H596 (lung adenosquamous carcinoma) cell line.

3.1.2. Prostate cell lines

3.1.2.a PC-3 cell line

The T75 flasks were seeded with approximately $9x10^4$/ml cells and the growing rate was monitored. As illustrated in figure 3.3, the lag phase had a duration of 48 hours. The peak of the exponential phase was reached after 240 hours of growth and the number of cells was approximately $2.14x10^6$/ml. The exponential phase was followed by a stationary period of nearly 48 hours and then the number of cells started decreasing.

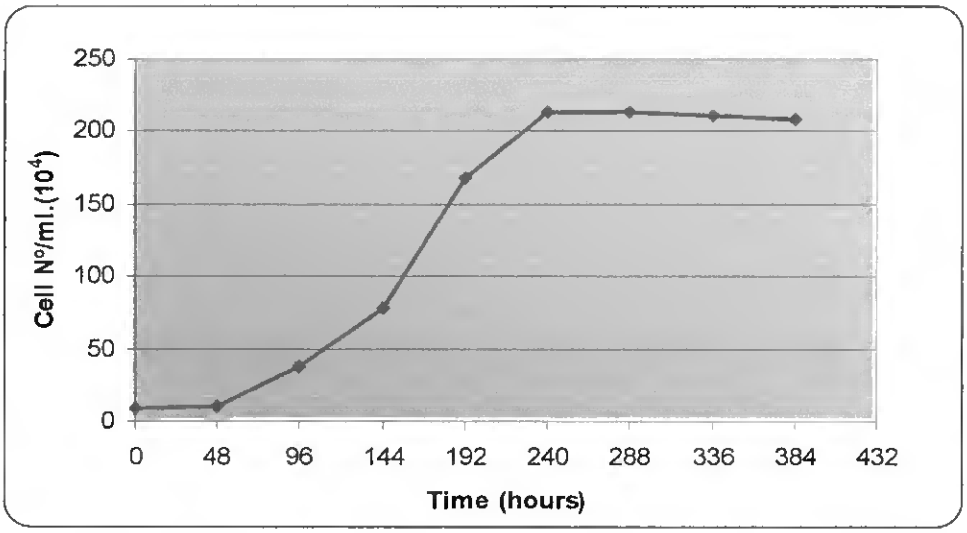

Figure 3.3 – Cellular proliferation of the PC-3 (prostate adenocarcinoma) cell line.

3.1.2.b PNT-1A cell line

The T25 flasks were seeded with approximately $9x10^4$/ml cells and the growing rate was monitored. Lag phase had a duration of nearly 24 - 48 hours, as illustrated in figure 3.4. The peak of the exponential phase was reached after 120 hours of growth and the number of cells was approximately $8.2x10^5$/ml. The stationary phase was practically non-existent and the number of cells began to decrease immediately after the exponential phase.

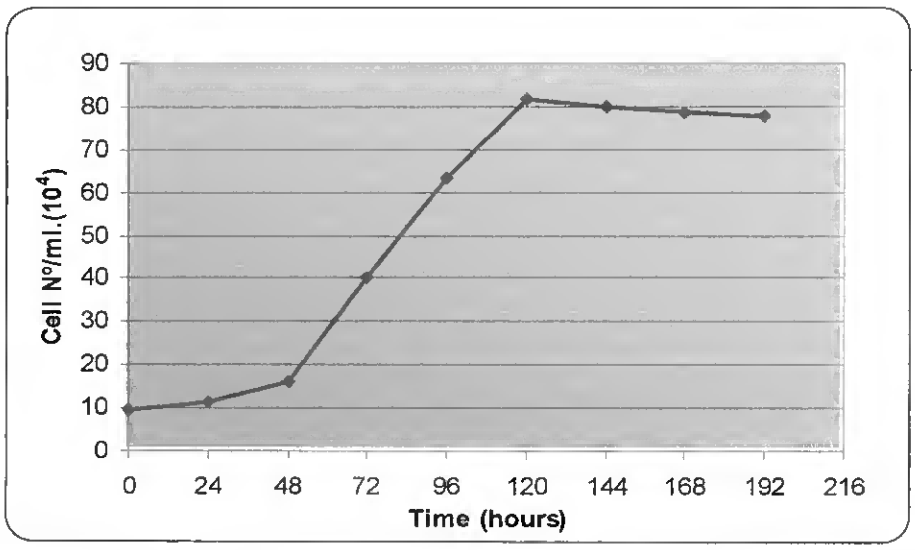

Figure 3.4 – Cellular proliferation of the PNT-1A ("normal" prostate) cell line.

3.2 – Cellular morphology

The morphological differences between cancer and normal cells were clearly observed *in vitro* and recorded using a light microscope (Nikon, Japan) and a digital camera (Olympus, China). The images were obtained by using the microscope eye piece of 10x magnification, and the 10x and 20x phase objectives.

3.2.1. Lung cell lines

3.2.1.a HBE 135-E6E7 cell line

The HBE135-E6E7 cell line, "normal" lung cells, grew as a uniform monolayer. The cells tended to be rounded when the confluence in the flask was low, figure 3.6a. However, when a confluence of 100% was achieved, the cellular monolayer was formed by juxtaposed and polyhedron shape cells, with high cohesion, as shown in figure 3.6b.

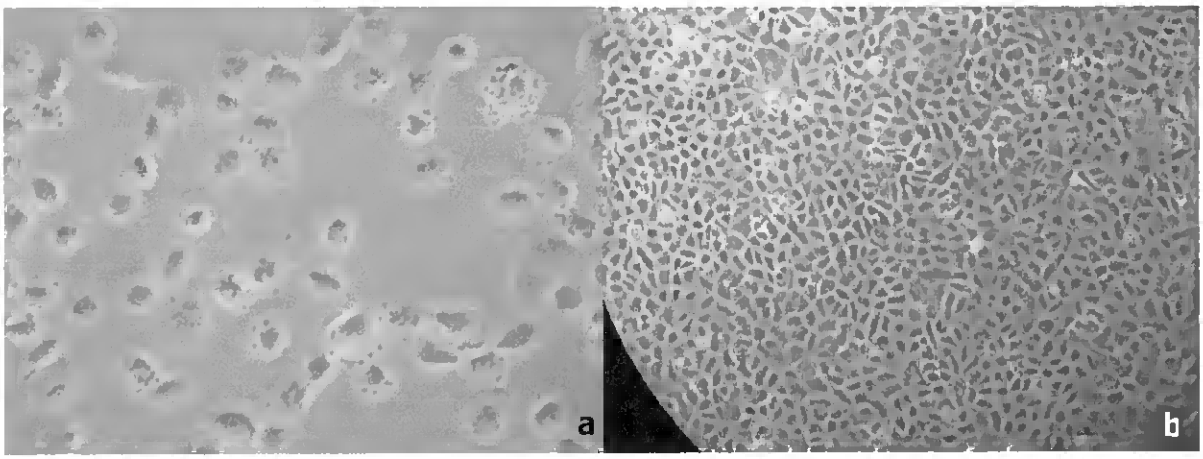

Figure 3.5 – Cellular morphology of HBE135-E6E7 cells. These cells represent the fifth passage of cellular growth. a) Image obtained using the 20x phase objective and representing a cellular confluence of approximately 50%. b) Image obtained using the 10x phase objective and representing a cellular confluence of 100%.

This cell line also exhibited a number of cells that appeared to have apoptotic activity which is characterized by membrane blebbing and can be observed in figure 3.7 [45].

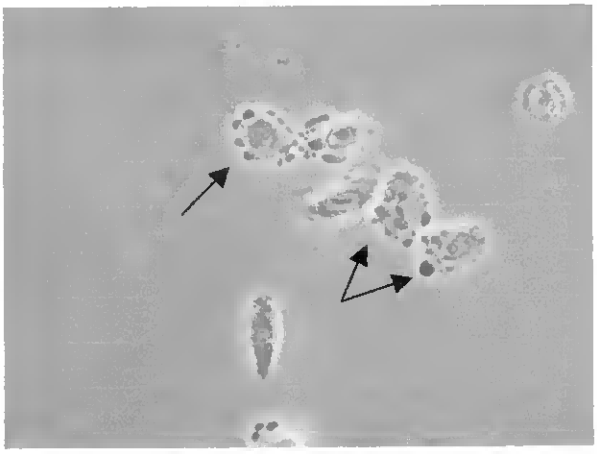

Figure 3.6 – Cellular morphology of apoptotic HBE135-E6E7 cells. These cells represent the fifth passage of cellular growth and this image was obtained using the 20x phase objective.

3.2.1.b NCI-H596 cell line

The NCI-H596 cell line, lung adenosquamous carcinoma, is characterized by different types of cell morphologies, as illustrated in figures 3.5a and b. In figure 3.5a, the blue arrow refers to the cells that grew as a group and which appeared to be of smaller dimensions than the surrounding cells and the red arrows indicate the cells which appeared to have a polyhedron shape as an epithelium. The spherical cell pointed by the pink arrow indicates a cell that probably did not have enough space to attach and to grow on the surface of the flask because the confluence was already 100%. Relative to the figure 3.5b, the yellow arrows refer to the cells which were elongated and presented an especially irregular morphology, and the green arrow is pointing an enlarged cell with various projections and large nuclei.

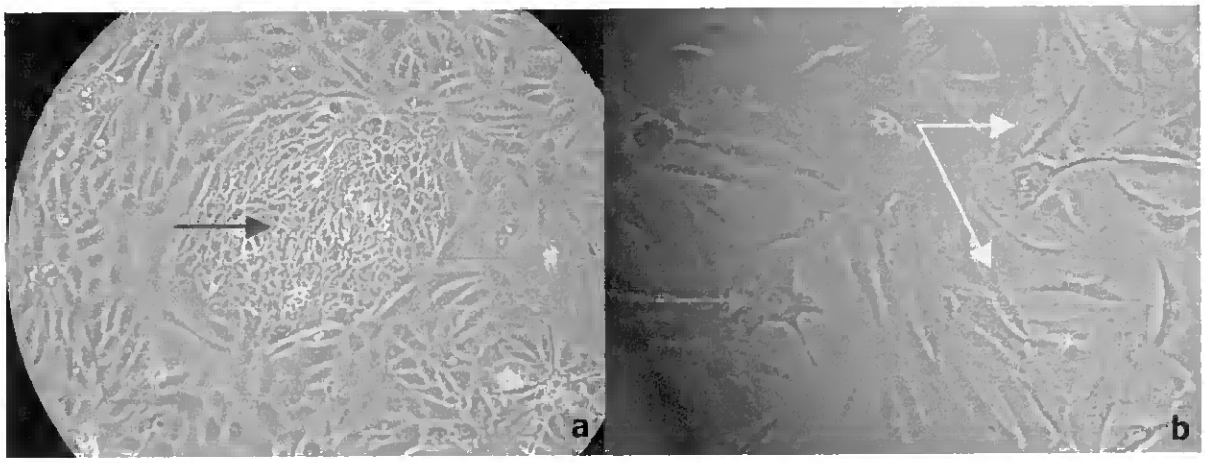

Figure 3.7 – Cellular morphology of NCI-H596 cells. These cells represent the seventh passage of cellular growth. a) Image obtained using the 10x phase objective and representing a cellular confluence of 100%. b) Image obtained using the 20x phase objective and representing a cellular confluence of 100%.

3.2.2. Prostate cell lines

3.2.2.a PC-3 cell line

The PC-3 cell line, prostate adenocarcinoma, exhibited an extremely irregular morphology, as shown in figures 3.8a and b. Some cells, like the ones indicated by the red arrows were morphologically elongated and thin. The blue arrows indicate cells that were rounded and enlarged, and the pink arrows indicate cells that were morphologically similar to fibroblasts because they were spindle-like. Generally, PC-3 cells exhibited a large nucleus.

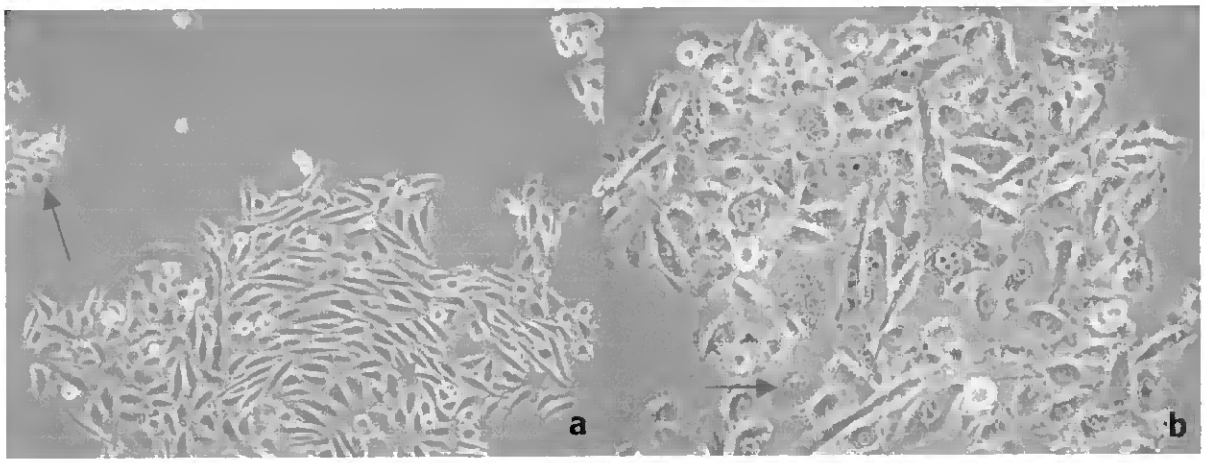

Figure 3.8 – Cellular morphology of PC-3 cells. These cells represent the sixth passage of cellular growth. a) Image obtained using the 10x phase objective and representing a cellular confluence of 30%. b) Image obtained using the 20x phase objective and representing a cellular confluence of 50%.

In order to demonstrate that the spherical cells in figure 3.9a indicated by black arrows were characteristic from this cell line and not due to the high number of passages (twenty two), figures 3.9b and c have been included for reference (ATCC – American Type Culture Collection) [43].

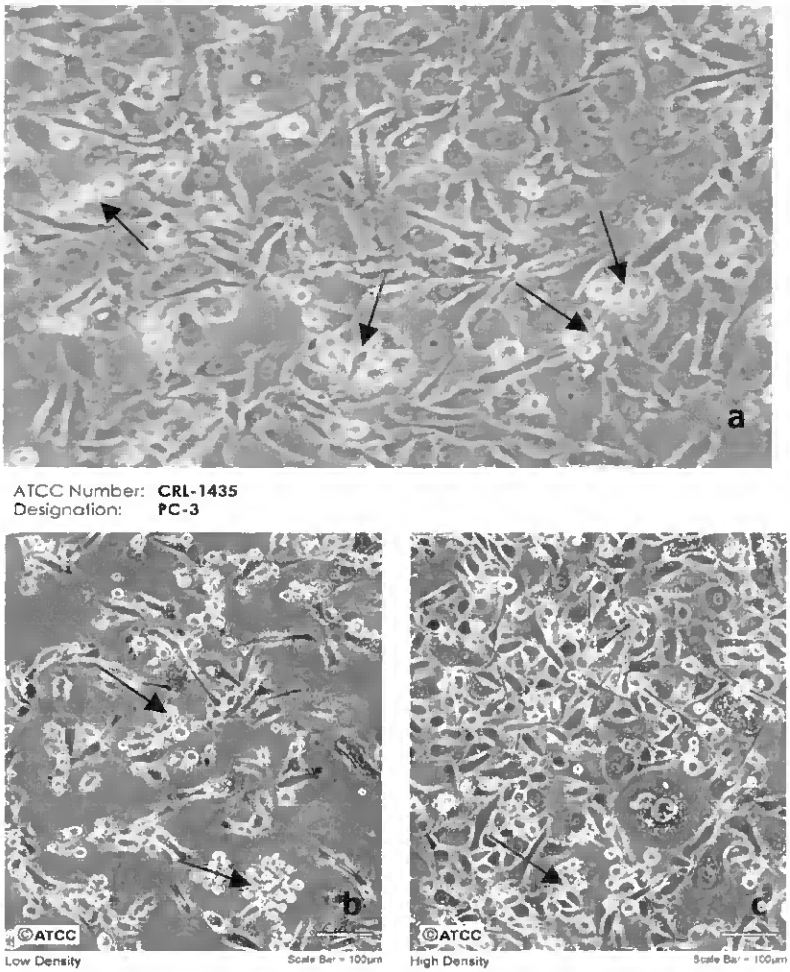

Figure 3.9 – Cellular morphology of PC-3 cells. a) These cells illustrate the twenty second passage of cellular growth with a confluence of almost 100%. The image was obtained using the 20x phase objective. b) Image obtained from the ATCC catalogue showing a low density of cells. c) Image obtained from the ATCC catalogue showing a high density of cells.

3.1.2.b PNT-1A cell line

The PNT-1A cell line, "normal" prostate cells, grew in a uniform monolayer. The cells looked flattened, slightly elongated and spindle-like as illustrated in figure 3.10a) and b) and indicated by the black arrows.

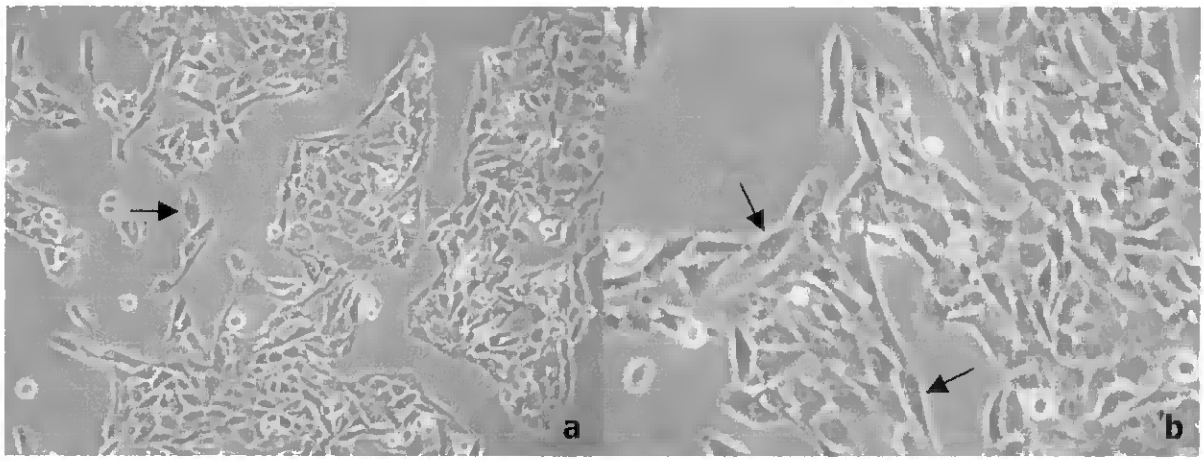

Figure 3.10 – Cellular morphology of PNT-1A cells. These cells represent the eighth passage of cellular growth. a) Image obtained using the 10x phase objective and representing a cellular confluence of 70%. b) Image obtained using the 20x phase objective and representing a cellular confluence of 70%.

It was also generally observed that as confluence increased to 100% the number of cells attached to the flask started decreasing and the number of dead floating cells and debris started increasing. However, this appeared to happen faster in both "normal" cell lines than in cancer cell lines.

3.3 – Nucleic acids amplification

3.3.1. PCR optimization

During the polymerase chain reaction, DNA is amplified by a series of polymerization cycles consisting of three temperature-dependent steps: DNA denaturation, primer-template annealing and DNA synthesis by a thermostable DNA polymerase. The purity and yield of the reaction products depend on several parameters, which are magnesium concentration, buffer composition, enzyme choice and concentration, primer design, amount and quality of the template DNA and cycle parameters as the annealing temperature. In this study, in order to optimize amplification of the desired PPIA pseudogene genomic sequence (491bp), three different annealing temperatures (Ta) were tested as described in chapter 2.

Firstly, the reaction was tested using 52ºC as annealing temperature and the products were run on a 1% (w/v) agarose gel which was then stained in ethidium bromide. The results are illustrated in figure 3.11.

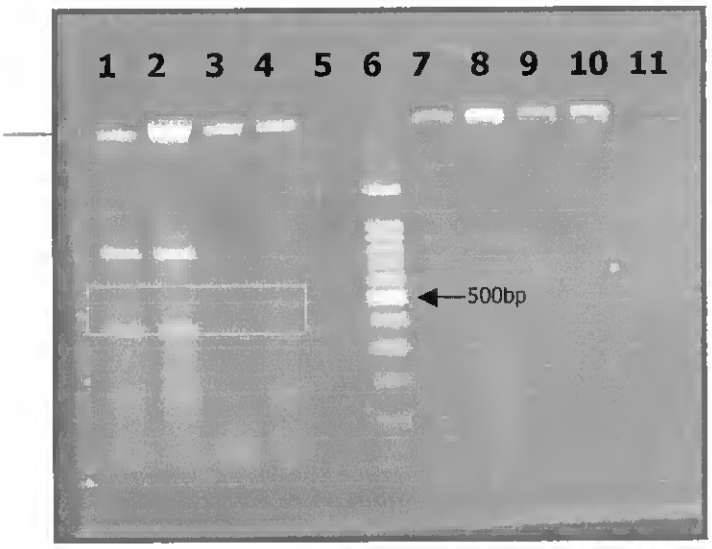

Figure 3.11 – PCR products in 1% (w/v) agarose gel stained in ethidium bromide showing several non-specific bands. The amplification was performed using an annealing temperature of 52ºC. Lanes 1, 2, 7 and 8 represent DNA from PC-3 cells and lanes 3, 4, 9 and 10 represent DNA from PNT-1A cells. Lanes 1 to 5 are the products of reactions performed with 10xPCR buffer. Lanes 7 to 11 are the products of reactions performed with 10xCoralLoad PCR buffer. Lanes 5 and 11 are negative controls and lane 6 is a 100bp DNA ladder.

In order to test both PCR buffers supplied with the Qiagen Taq PCR Core kit (Qiagen, Crawley, UK), reactions on the left side of the ladder were performed with Qiagen 10x PCR buffer and on the right side with the Qiagen 10x CoralLoad PCR buffer. The advantage of using the later is that it allows direct electrophoresis of the PCR products without the addition of loading buffer to the PCR. The reactions 1 and 7, 2 and 8, 3 and 9, and 4 and 10 were performed with the same DNA templates however, with 10x PCR buffer, practically no bands were obtained. Only the bands on the top of the gel indicated by the red arrows are visible and which are high molecular weight genomic DNA template. These bands are also observed with 10x PCR buffer.

The gel showed that several non-specific amplification reactions occurred. These were mainly visible in lanes 1 and 2 from PC-3 template DNA. In lanes 3 and 4 from PNT-1A template DNA, the bands were almost not visible except for a high molecular weight band. This fact is probably due to the small amount of DNA that was placed into the reaction tube. In lanes 1, 2 and 4 it was possible to see a feint band (orange box in the figure 3.11) of approximately 500bp which probably represents the PPIA sequence.

In order to increase specificity, the annealing temperature was increased to 58ºC and the results are shown in figure 3.12. Lane 1 containes a 100bp ladder, lanes 2 and 3 contain DNA from PC-3 cells, lanes 4 and 5 contained DNA from

PNT-1A cells and lane 6 was the negative control. Practically no PCR products were visible except for a low molecular weight band which also appeared in the negative control. This was probably the result of cross contamination between samples.

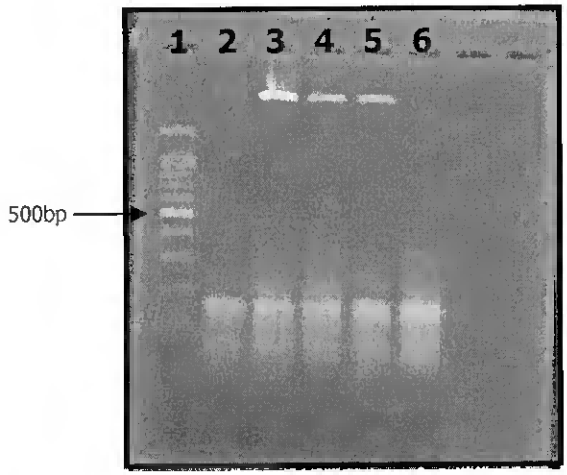

Figure 3.12 – PCR products in 1% (w/v) agarose gel stained in ethidium bromide. The amplification was performed using an annealing temperature of 58°C. Lane 1 is a 100bp DNA ladder. Lanes 2 and 3 represent DNA from PC-3 cells and lanes 4 and 5 represent DNA from PNT-1A cells. Lanes 6 is the negative control.

After observing that an annealing temperature of 58°C failed to produce PCR products, the reaction was tested again with a different temperature, 55°C. By looking at the electrophoresis gel, figure 3.13, it was possible to visualize that only one band was present for the expected PCR products. This corresponded to 500bp and meant that the PCR was optimized.

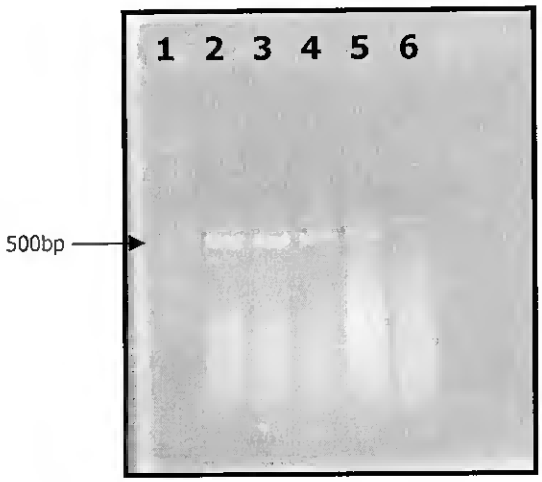

Figure 3.13 – PCR products in 1% (w/v) agarose gel stained in ethidium bromide. The amplification was performed using an annealing temperature of 55°C. Lane 1 is a 100bp DNA ladder. Lanes 2 and 3 represent DNA from PC-3 cells and lanes 4 and 5 represent DNA from PNT-1A cells. Lanes 6 is the negative control.

3.4 – PPIA pseudogene mRNA expression

Reverse Transcriptase – Polymerase Chain Reaction (RT-PCR) is a technique developed to measure gene expression in tissues and cells and which was used in this study to determine the presence or absence of a transcript for the PPIA pseudogene in lung and prostate cell lines.

In order to select the most appropriate primer to perform the reverse transcription of the mRNA into cDNA, both Oligo(dT)20 and random-hexamer primers, supplied with the Cloned AMV First-Strand cDNA Synthesis Kit (Invitrogen, Paisley, UK), were tested, and those reactions are illustrated in figure 3.14.

Lane 1 is a 100bp DNA ladder, lanes 2 and 3 represent amplified cDNA from NCI-H596 cells, lanes 4 and 5 from HBE135-E6E7 cells and lanes 6 and 7 from PC-3 cells. Lane 8 is the negative control which represents an RT-PCR reaction performed with all the reagents, mentioned in chapter 2, but RNA template and lane 9 is the positive control using genomic DNA from NCI-H596 with β-actin primers. The reverse transcriptase step relative to reactions 2, 4 and 6 were performed with Oligo(dT)20 primers while reactions 3, 5 and 7 with random-hexamer primers. Relative to the PCR step, the reactions 2 to 5 were performed with gene specific primers and, the reactions 6 and 7 with the β-actin primers.

Only a small band of nearly 200bp, was visible, looking slightly brighter in lanes 3 and 5, which correspond to the use of random-hexamer primers. The β-actin primers worked with genomic DNA from NCI-H596 cells but not with cDNA from PC-3 cells which led to the placement of a higher amount of RNA sample into the RT reaction tube in the following reaction.

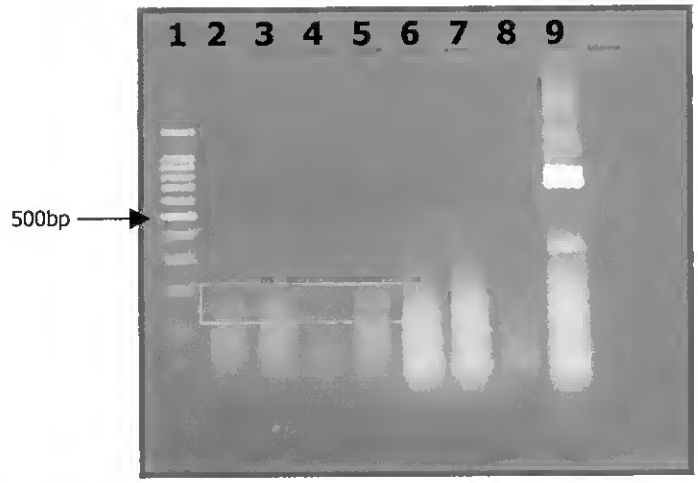

Figure 3.14 – RT-PCR products in 1% (w/v) agarose gel stained in ethidium bromide. Lane 1 is a 100bp DNA ladder. Lanes 2 and 3 represent $_{total}$RNA from NCI-H596 cells reverse transcribed into cDNA with Oligo(dt)20 and random-hexamer primers respectively. Lanes 4 and 5 represent cDNA from HBE135-E6E7 cells reverse transcribed with Oligo(dt)20 and random-hexamer primers respectively. Lanes 6 and 7 represent cDNA from PC-3 cells reverse transcribed and amplified with B-actin primers respectively. Lane 8 is the negative control and lane 9 represent NCI-H596 DNA amplified with B-actin primers.

Finally, it was decided to test the random-hexamer primers again along with the gene specific primer. The results of those reactions are presented in figure 3.15.

Lanes 1 and 13 are a 100bp DNA ladder, lanes 2 to 4 represent cDNA from NCI-H596 cells, lanes 5 and 6 from HBE135-E6E7 cells, lanes 7 and 8 from PC-3 cells, lanes 9 and 10 from PNT-1A cells, lane 11 is the negative control and lane 12 is the positive control which reaction amplified genomic DNA from NCI-H596 with β-actin primers. The reverse transcriptase reactions 2, 5, 7 and 9 were performed with random-hexamer primers and the reactions 3, 6, 8 and 10 with the gene specific primer. With respect to the PCR, reactions 2, 3 and 5 to 10 were performed with gene specific primers and reactions 4 and 12 with the β-actin primers.

In the end of the gel it was possible to visualize a band of approximately 100 bp which is not correspondent to the PPIA pseudogene expression. This band appears to be slightly brighter in the reactions where the gene specific primer was used as it is possible to observe in lanes 3, 6, 8 and 10.

In lane 12 it was possible to observe an extremely bright band, blue box, corresponding to the β-actin genomic DNA and in lane 4 a band with approximately 650bp corresponding to the β-actin expression, pink box, which could prove that the RT step was working. However, due to lack of time it was not possible to optimize the conditions of the RT-PCR in order to be absolutely sure whether or not the PPIA pseudogene was being expressed in the remaining cell lines.

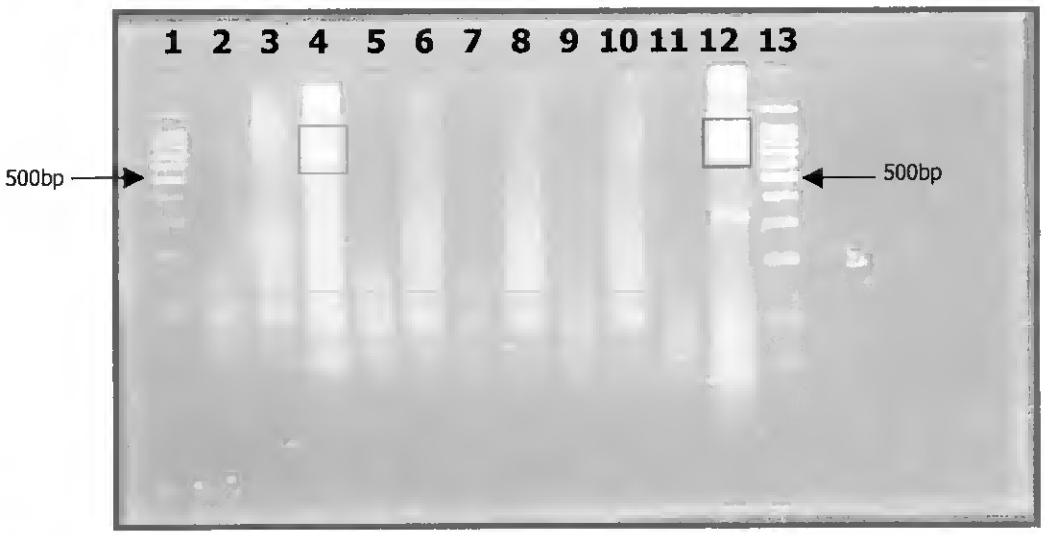

Figure 3.15 – RT-PCR products in 1% (w/v) agarose gel stained in ethidium bromide. Lanes 1 and 13 are the 100bp DNA ladder. Lanes 2 and 3 represent mRNA from NCI-H596 cells reverse transcribed into cDNA with random-hexamer and gene specific primers respectively. Lane 4 represents the positive control with β-actin primers and NCI-H596 mRNA. Lanes 5 and 6 represent mRNA from HBE135-E6E7 cells reverse transcribed into cDNA with random-hexamer and gene specific primers respectively. Lanes 7 and 8 represent mRNA from PC-3 cells reverse transcribed into cDNA with random-hexamer and gene specific primers respectively. Lane 9 and 10 represent mRNA from PNT-1A cells reverse transcribed into cDNA with random-hexamer and gene specific primers respectively. Lane 11 is the negative control and lane 12 represent NCI-H596 DNA amplified with β-actin primers.

Chapter 4 – Discussion

This chapter will be focussed on discussing the results, aims and objectives of this study which had the purpose of studying and comparing the cellular proliferation and morphology between cancer and "normal" cells of lung and prostate. On addition, the aim was to investigate the presence and expression of the PPIA pseudogene in a particular cell line of lung cancer (NCI-H596) and its expression in other cell lines.

4.1 – Cellular proliferation

The analysis of the cellular proliferation growth curves allows the comparison between cancer and normal cellular growth which exhibit some differences.

Both lung cell lines exhibited a lag phase of 48 hours and an exponential phase of 96 hours. The cancer cell line (NCI-H596) achieved the maximum confluence of $4.6x10^5$ cell/ml and the normal cell line (HBE135-E6E7), $3.5x10^5$ cells/ml. The stationary phase of lung cancer cells was more prolonged than the stationary phase of "normal" lung cells which was almost inexistent once the cell number started to decrease after achieving the peak of the exponential phase. Those events may be due to the higher level of contact inhibition that may happen between "normal" cells.

The comparison between the prostate cells growth is slightly more difficult, because the cells grew on different surface areas. The PC-3 cells were seeded and grown in T75 flasks and the PNT-1A cells in T25 flasks which appeared to nearly double the growth time of the PC-3 cells. Prostate cancer cells had a lag phase of 48 hours while "normal" cells had a lag phase of 24-48 hours demonstrating that they started proliferating earlier than PC-3. However, they both reached the peak of exponential phase at the same equivalent time. While the PNT-1A cell line reached a maximum number of cells of $8.2x10^5$/ml in 120 hours after seeding, PC-3 cell line reached the peak of confluence in 240 hours, doubling the time taken to obtain a maximum of $8.2x10^5$ cells/ml. Meaning that with approximately the same time of growth, PC-3 cell line reached a higher number of cells, even having a lag phase 24 hours longer.

As it was verified with lung cells, the prostate cancer cell line also exhibited a more prolonged stationary phase when compared to the prostate "normal" cell line. While PC-3 cells maintain approximately the same number of cells during the next 48 hours after the peak, the number of PNT-1A cells started decreasing after reached the peak. This may be due to the same reason given above, the greater level of contact inhibition that may be occurring between "normal" cells.

Comparing the proliferation of both lung cells and both prostate cells, it was possible to understand that prostate cells grew faster and reached a greater degree of confluence than lung cells.

4.2 – Cellular morphology

The comparative morphology of normal and cancer cells showed that there are some phenotypic differences between them.

NCI-H596 lung cells and PC-3 prostate cells exhibited a wide variety of morphologies which is most probably a property of all types of cancer cells. Both cancerous cell lines showed disorganized growth patterns, while HBE135-E6E7 lung cells and PNT-1A prostate cells which are representative of normal cells demonstrated a regular pattern of growth. Another factor that may have contributed to the higher number of cells achieved with both cancer cell lines in the end of the exponential phase, and the relatively short stationary phase obtained by the "normal" cell lines is the slightly larger size of the "normal" cells compared to the cancer cells. This together with the fact that normal cells are anchorage dependent, probably stopped the cells dividing because of the lack of space necessary to continue growing on the surface of the flask and consequently the number of dead floating cells and debris increased.

As described in the results chapter, HBE135-E6E7 cell line grew as a uniform monolayer and when a high level of confluence was reached, the cells formed a layer of juxtaposed and polyhedron shape cells, with high cohesion. This polyhedron-like morphology is due to the high number of desmosomes present in the plasma membranes of the cells which are cellular junctions acting as mediators of cellular organization [45]. This cell line also exhibited some blebbing which is indicative of apoptotic activity, figure 3.7, but in the opposite way this occurrence happens because of the lesser amount of desmosomes in the plasma membrane [46].

Comparing figure 3.9a) and figures 3.9b) and c) it IS possible to understand that the spherical and unanchored cells are characteristic of the PC-3 cell line even when the confluence is not 100%. Probably it is their attempt to form clusters as they possess that property when cultured in soft agar [42].

As mentioned before, there is another event that may have also contributed to stop the cell division and consequently provoked cell death and which is named "contact inhibition". This effect is controlled by cadherins and catenins which participate in transduction of extracellular signals that control cell proliferation, migration and differentiation, and it is produced when epithelial cells contact each other provoking the formation of adherent junctions, and suppressing the normal cell proliferation [45], [47] .

4.3 – Nucleic acids amplification

4.3.1. PCR optimization

PCR is one of the most used techniques in molecular biology, and, in spite of its simple principle, PCR can be difficult to optimize. Normally, several experiments are required to achieve optimal conditions for PCR, even if good primers are chosen. Optimization of PCR involves testing a number of variables and one of which is the annealing temperature (Ta), required at the primer-template annealing step and critical when total genomic DNA is the substrate for PCR [48].

In this study, in order to know the most appropriate annealing temperature, three different temperatures were tested using genomic DNA from PC-3 and PNT-1A cell lines. Initially, when a Ta of 52°C was used, figure 3.11, non-specific DNA fragments were amplified, causing the appearance of multiple bands on the agarose gel. In order to increase specificity, a high annealing temperature of 58°C was tested. As shown in figure 3.12 practically no bands were visible on the gel which probably was the result of poor annealing of the primers as the temperature was too high. Finally, it was necessary to try a lower temperature, 55°C. By observation of the gel, figure 3.13, it was possible to visualize the presence of only one band corresponding to practically 500bp length sequence which suggest that the primers were annealing with the DNA template at this temperature and with high specificity considering that the desired PPIA pseudogene sequence has a length of 491bp [48].

The analysis of the gel illustrated by figure 3.11 allowed concluding that the Qiagen 10x CoralLoad PCR buffer did not work as mentioned in the kit specifications as no bands on the right side of the gel were visible. The bands present on the top of the same gel and on the top of the gel illustrated by figure 3.12 were not visible on the other gels and which were most probably provoked by a small amount of template that came out of the well after pipetting.

In some of the electrophoresis gels presented in the results it was visible in the end of the lanes an increased smearing which could be due to the use of non-calibrated pipets and which consequently were pipetting a higher amount of primers than the actual needed, or could also be degraded template.

4.3.2. PPIA pseudogene mRNA expression

Reverse transcriptase – polymerase chain reaction (RT-PCR) was the technique used during this work to study the presence or absence of a transcript, i.e., to study whether or not the PPIA pseudogene is being expressed in all the cell lines studied.

In order to select the appropriate primer to synthesise the cDNA during the RT step, the three types of primers, oligo(dT)20, random-hexamer and gene specific primers, were tested. However, with all of them the results were poor as only a feint band of the wrong size was obtained in the end of the gels and mainly with the gene specific primer, figures 3.14 and 3.15. In figure 3.15, a band in lane 4 was seen with approximately 650bp corresponding to the β-actin expression (positive control), which suggests that the RT step was working. However it is known that β-actin is a very abundant transcript in human cells and which is easily amplified even when the RT conditions are not the ideal. Thus, its presence in the gel does not prove with 100% certainty that the RT conditions were the appropriate to amplify the PPIA pseudogene sequence.

It was not possible to optimize the RT-PCR conditions in order to be absolutely sure whether or not the PPIA pseudogene was being expressed. A number of physical and chemical factors should be considered during the selection of the optimal system in order to perform the reaction with fidelity.

The splicing pattern of the pseudogene sequence is unclear, but it was noticed that one of the gene specific primers could be specific to anneal to part of an intron sequence instead of an exon. This possible issue can have compromised all

the expression results as one of the primers would not be effective and would provoke the failure of the RT-PCR protocol. In order to solve this problem, further studies would have to look at the splicing of the desired sequence and design a new gene specific primer which would anneal to the exon sequence. This fact means that it would be necessary to proceed with a new PCR optimization in order to know which temperature would be the ideal for the primers-template annealing.

The size and secondary structure of the target mRNA is also an important factor for the RT step. If the secondary structure of the PPIA pseudogene mRNA was known, a possible optimization to the protocol could be the designing of a gene specific primer which could be extended through significant secondary structure of the mRNA [49].

Figure 4.1 is related to the optimization of the RT-PCR conditions used by Salto et al. (1999) [49]. The image of the electrophoresis gel represents the amplification of the PCR products with increasing numbers of PCR cycles. The PCR products were collected before the reaction began to reach the plateau phase and then, the amount of mRNA amplified in each sample was quantified by densitometry and plotted against the cycle number in order to construct the optimization curve which serves as DNA quantification control. This procedure is performed with the objective of knowing if all the samples are within the lineal range of the optimization curve and could be used during the optimization process [49].

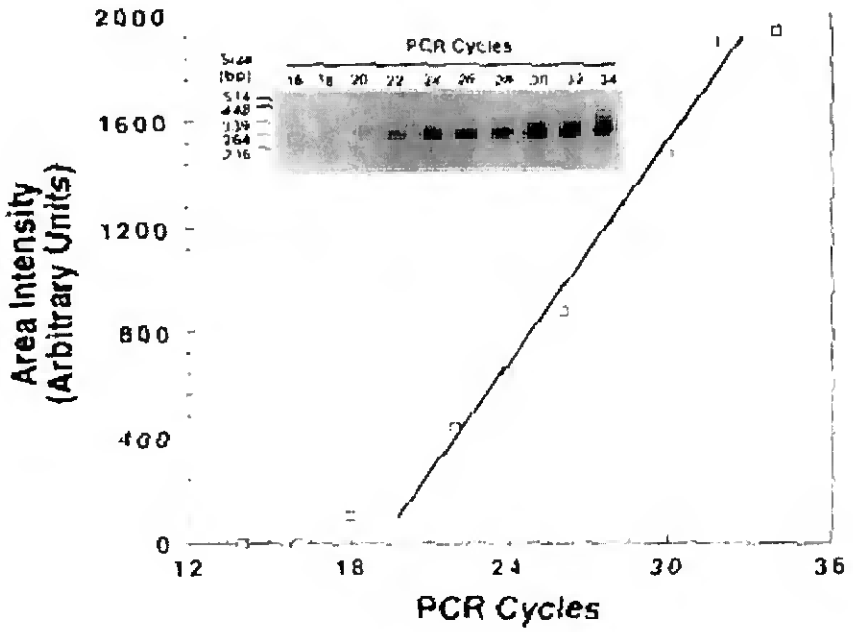

Figure 4.1 — Optimization of RT-PCR conditions. An image of PCR products amplified with increasing numbers of PCR cycles is shown at top of the panel. PCR products were separated by electrophoresis in 2% agarose gels and stained with ethidium bromide. The amount of mRNA amplified in each sample was quantified by densitometry and plotted against the cycle number [49].

As probably there was no synthesis of target cDNA, the integrity of the RNA should be verified by denaturing agarose gel electrophoresis and/or the concentration of template RNA could be increased. During the RNA extraction the RT inhibitors could be removed by an additional 70% ethanol wash after ethanol precipitation [50], [51].

After the optimization of the RT-PCR conditions there are several scenarios that could be obtained as results. The PPIA gene is normally expressed in human cells and so a band representing its transcript should be obtained even if the PPIA pseudogene is not expressed. Another possible option is the expression of the PPIA pseudogene in the NCI-H596 cell line where the sequence was found to be altered, and not in the other cell lines. Finally, the expression could also be observed in all cell lines with no difference in level. If the third option was true it would be necessary to study the relation and function of the PPIA pseudogene in lung cancer.

In order to know and identify what are the RT-PCR products some other techniques could be performed. DNA sequencing is one of those and which is a powerful technique used in molecular biology. The determination of the DNA sequence is the only method which generates information that is not based on hypotheses. Thus, it would be a good technique to scan the sequences amplified during the RT-PCR and then detect the presence or not of the single nucleotide mutation. The technique is based on the principle that single-stranded DNA molecules which differ in length by just a single nucleotide can be separated from one another using polyacrylamide gel electrophoresis [52].

Northern blotting is still a popular method for analysis of gene expressions in which the splicing pattern is unclear or alternative and should be considered as an efficient alternative to RT-PCR. As probably this fact illustrates the current case study and even knowing that it is a time-consuming and costly technique this conventional RNA blotting method should be applied for the analysis of the PPIA pseudogene expression. This technique also provides information about mRNA size and the integrity of RNA samples and it is performed by transferring the RNA species separated in electrophoretic gels to membrane filters for detection and identification of specific base sequences by complementary probes [53], [54].

However to quantify the levels of expression the ribonuclease protection assay could be performed. The principle of this technique is based on the hybridization in solution of a radiolabeled complementary *in vitro* transcript probe

and target RNA. Then, the solution is treated with ribonuclease in order to degrade all remaining single-stranded RNA and the hybridized portion of the probe will be protected from digestion. The ribonuclease protection assay products are then visualized by performing an electrophoresis of the mixture on a denaturing polyacrylamide gel followed by autoradiography. The RNA can be then quantified by direct relation to the amount of radiolabeled probe hybridized [55].

The ribonuclease protection assay is an extremely sensitive technique for the quantification of specific RNAs in solution and according to Ekenberg, S. et al. (1994) it is a superior technique to Northern blotting for the detection and quantification of low abundance RNAs. With blotting, RNA transference and binding to the membrane during the performance of the Northern blotting may be inefficient and once bound, some RNA molecules may not be accessible for hybridization. Another disadvantage of using Northern blotting is the fact that sample integrity influences the degree to which the signal is localized in a single band [55]. The ribonuclease protection assay can also be useful for mapping transcript initiation and termination sites and intron/exon boundaries, and for discriminating between related mRNAs of similar size, which would migrate at similar positions on a northern blot. This feature would be an advantage for further studies as the transcript initiation and termination sites and intron/exon boundaries are unknown for the PPIA pseudogene [54].

Another methodology that could be used to identify the RT-PCR products is the Southern blotting and hybridization as it was shown that RT-PCR assays using this procedure are more sensitive than those using agarose gel detection. This technique is based on the same principle as the one used in Northern blotting [25]. Could also be used the Real time PCR technique and would not be necessary to perform the electrophoresis technique as this methodology allows for the direct detection of RT-PCR product during the exponential phase of the reaction, by combining amplification and detection in a single step [56].

Chapter 5 – Conclusion

In the end of this study not all of the objectives were achieved.

Both lung cell lines exhibited a similar cell proliferation, reaching the end of the lag phase and the peak of the exponential phase at the same time. However, cancer cells obtained a higher number of cells in the end of the stationary phase which was more prolonged. Those observations allowed the conclusion that the contact inhibition effect is higher in normal cells than in cancer cells. The slightly larger size that "normal" cells showed may also contribute to that occurrence. Practically the same proliferation trend was observed with the prostate cell lines, the difference being that the "normal" cell line had a shorter lag phase.

It was also possible to conclude that "normal" cells are anchor-dependent as they stopped dividing when high confluence was reached because there was no free space in the surface flask where they could continue growing.

Both prostate cell lines grew faster than lung cell lines.

Cancer cells exhibited a wide variety of cellular morphology when compared to "normal" cells. Both lung and prostate cancer cells did not show cell homogeneity during the growth, unlike the "normal" cells, which grew as a uniform monolayer. This characteristic of cancer cells is due to the fact that they acquired disorganized growth patterns after being "naturally" transformed.

The optimization of the PCR was reached, as the annealing temperature was optimized to 55ºC in order to test the primers viability to amplify the PPIA pseudogene genomic sequence.

The expression of the PPIA pseudogene was not demonstrated for a number of reasons. Probably the primers would have to be designed again in order to make sure that they are specific for the exon sequence and the other RT conditions would have to be optimized. Also would be most favourable to the continuation of the study the performance of DNA sequencing in order to identify the PPIA pseudogene mRNA.

References

[1] CancerIndex:
http://www.cancerindex.org/clinks14.htm (accessed: 8 August 2006)

[2] Souhami, R. & Tobias, J. (2005) Cancer and its management. Blackwell Publishing, 5th Edition, 1.

[3] Jemal, A., Murray, T., Ward, E., Samuels, A., Tiwari, R., Ghafoor, A., Feuer, E., & Thun, M (2005) Cancer Statistics, 2005. Cancer Journal for Clinicians 55, 10-30.

[4] Ruano-Ravina, A., Figueiras, A. & Barros-Dios, J. M. (2003) *Lung cancer and related risk factors: an update of the literature.* Elsevier, Journal of the royal institute of public health 117, 149 – 156

[5] Cancer Information Network:
http://patient.cancerconsultants.com/lung_cancer_news.aspx?id=23597 (accessed: 14 June 2006)

[6] Haura, E. B. (2006) *Is repetitive wounding and bone marrow-derived stem cell mediated-repair an etiology of lung cancer development and dissemination?* Elsevier, Medical hypotheses 67 (4), 951-956.

[7] Cancer Research UK:
http://info.cancerresearchuk.org/cancerstats/types/lung/incidence/ (accessed: 12 June 2006)

[8] Cancer Research UK:
http://www.cancerhelp.org.uk/help/default.asp?page=2964 (accessed: 20 July 2006)
[9] Cancer Research UK:

http://www.medicinenet.com/lung_cancer/article.htm (accessed: 20 July 2006)

[10] Cancer Research UK:
http://www.cancer.org/docroot/CRI/content/CRI_2_4_3X_How_is_cancer_of_unknown_primary_diagnosed_58.asp (accessed: 20 July 2006)

[11] Pass, H. I., Mitchell, J. B., Jonhson D. H., & Turrisi, A. T. (1996) *Lung Cancer – Principles and Practice.* Lippincott – Raven Publishers

[12] van Gils, M. P., Stenman, U. H., Schalken, J. A., Schroder, F. H., Luider, T. M., Lilja, H., Bjartell, A., Hamdy, F. C., Pettersson, K. S., Bischof, R., Takalo, H., Nilsson, O., Mulders, P. F. & Bangma, C. H. (2005) *Innovations in Serumand UrineMarkers in Prostate Cancer Current European Research in the P-Mark Project.* European Urology 48, 1031–1041.

[13] Klein, E. A. (2005) *Chemoprevention of prostate cancer.* Critical Reviews in Oncology/Hematology 54, 1–10.

[14] Abate-Shen, C. & Shen, M. M. (2000) *Molecular genetics of prostate cancer.* Genes & Development 14, 2410-2434.

[15] Tombal, B. (2006) Over- and Underdiagnosis of Prostate Cancer: The Dangers. Elsevier, European urology supplements 5, 511–513.

[16] Cancer Research UK: http://www.cancerhelp.org.uk/help/default.asp?page=2720 (accessed: 20 July 2006)

[17] Vermeulen, K., Van Bockstaele, D. R. and Berneman, Z. N. (2003) *The cell cycle: a review of regulation, deregulation and therapeutic targets in cancer.* Cell Proliferation 36, 131–149.

[18] Ratledge, C. & Kristiansen, B. (2001) *Basic Biotechnology.* Cambridge University Press, Second Edition, 449.

[19] Golias, C. H., Charalabopoulos, A. & Charalabopoulos, k. (2004) *Cell proliferation and cell cycle control: a mini review.* International journal of clinical practice 58 (12), 1134-1141.

[20] Israels, E. D. & Israels, L. G. (2001) *The Cell Cycle.* Stem Cells - Fundamentals of Cancer Medicine 19, 88-91.

[21] Zhu, M. H., Ni, C. R., Zhu, Z., Li, F. M. & Zhang, S. M. (2003) *Immunohistochemical demonstration of cyclins A,B,D1,D3 and E in hepatocellular carcinomas using tissue microarrays.* Zhonghua bing li xue za zhi, Chinese journal of pathology 32 (5), 440–3.

[22] Zhou, Q., He, Q. & Liang, L. (2003) *Expression of p27, cyclin E and cyclin A in hepatocellular carcinoma and its clinical significance.* World Journal of Gastroenterology 9 (11), 2450-2454.

[23] Hanahan, D. & Weinberg, R. A. (2000) *The hallmarks of cancer.* Cell 100 (1), 57-70.

[24] van Horssen, R., ten Hagen, T. L., & Eggermont, A. M. (2006) *TNF-α in Cancer Treatment: Molecular Insights, Antitumour Effects, and Clinical Utility.* The Oncologist 11 (4), 397-408.

[25] Niklinski, J. & Hirsch, F. R. (2002) *Molecular approaches to lung cancer evaluation.* Elsevier, Lung Cancer 38, S9-S17.

[26] Sekido, Y., Fong, K. M. & Minna, J. D. (1998) *Progress in understanding the molecular pathogenesis of human lung cance*r. Elsevier, Biochimica et Biophysica Acta 1378, F21-F59.

[27] Tan, G., Chu, Y., Chen, J., & Li, H. (2006) *Genomic Instability in the Progression of Sporadic Nasopharyngeal Carcinoma.* Otolaryngology - Head and Neck Surgery 134 (1), 147-152.

[28] Reis-Filho, J. S., Simpson, P. T., Gale, T. & Lakhani, S. R. (2005) *The molecular genetics of breast cancer: The contribution of comparative genomic hybridization.* Elsevier, Pathology – Research and Practice 201, 713–725.

[29] Basik, M., Stoler, D. L., Kontzoglou, K. C., Bigas, M. A., Petrelli, N. J. & Anderson, G. R. (1997) *Genomic Instability in Sporadic Colorectal Cancer Quantitated by Inter-Simple Sequence Repeat PCR Analysis.* Genes, Chromosomes & Cancer 18, 19–29.

[30] Benavides, F., Zamisch, M., Flores, M., Campbell, M. R., Andrew, S. E., Angel, J. M., Licchesi, J., Sternik, G., Richie, E. R. & Conti, C. J. (2002) *Application of Inter–Simple Sequence Repeat PCR to Mouse Models: Assessment of Genetic Alterations in Carcinogenesis.* Genes, Chromosomes & Cancer 35, 299-310.

[31] Broomhead, D. (2006) *Evaluation of the genome wide effects of cigarette smoke constituents in vitro.* Cranfield University, Unpublished PhD thesis.

[32] Howard, B. A., Zheng, Z., Campa, M. J., Wang, M. Z., Sharma, A., Haura, E., Herndon, J. E., Fitzgerald, M. C., Bepler, G. & Patz, E. F. (2004) *Translating biomarkers into clinical practice: prognostic implications of cyclophilin A and macrophage migratory inhibitory factor identified from protein expression profiles in non-small cell lung cancer.* Elsevier, Lung Cancer 46, 313-323.

[33] Campa, M. J., Wang, M. Z., Howard, B., Fitzgerald, M. C. & Patz, E. F. (2003) *Protein Expression Profiling Identifies Macrophage Migration Inhibitory Factor and Cyclophilin A as Potential Molecular Targets in Non-Small Cell Lung Cancer.* Cancer Research 63, 1652-1656.

[34] Grzmil, M., Voigt, S., Thelen, P., Hemmerlein, B., Helmke, K. & Burfeind, P. (2004) *Up-regulated expression of the MAT-8 gene in prostate cancer and its siRNA-mediated inhibition of expression induces a decrease in proliferation of human prostate carcinoma cells.* International Journal of Oncology 24, 97-105.

[35] Lewin, B. (2004) *Genes VIII.* Pearson Prentice Hall, International Edition, 93 – 95.

[36] Harrison, P. M., & Gerstein, M. (2002) *Studying Genomes Through the Aeons: Protein Families, Pseudogenes and Proteome Evolution.* Journal of Molecular Biology 318, 1155-1174.

[37] Balakirev, E. S. & Ayala, F. J. (2003) *Pseudogenes: Are They "Junk" or Functional DNA?* Annual Review of Genetics 37, 123-151.

[38] Cooper, G. M. & Hausman, R. E. (2004) *The Cell: A Molecular Approach.* 3rd Edition, ASM Press.

[39] McPherson, M. & Moler, S. (2006) *PCR – The Basics.* Taylor & Francis Group, Second Edition, 185, 222-224.

[40] American Type Culture Collection
http://www.lgcpromochem-atcc.com/common/catalog/numSearch/numResults.cfm?atccNum=HTB-178#Propagation

[41] American Type Culture Collection
http://www.lgcpromochem-atcc.com/common/catalog/numSearch/numResults.cfm?atccNum=CRL-2741#Propagation

[42] American Type Culture Collection
http://www.lgcpromochem-atcc.com/common/catalog/numSearch/numResults.cfm?atccNum=CRL-1435#Propagation

[43] The European Collection of Cell Cultures
http://www.ecacc.org.uk/

[44] http://www.ruf.rice.edu/~bioslabs/methods/microscopy/cellcounting.html

[45] Smith & Wood (1996) *Cell Biology*. Chapman & Hall, 2nd edition, 163.

[46] Coleman, M. L., Sahai, E. A., Yeo, M., Bosch, M., Dewar, A. & Olson, M. F. (2001) *Membrane blebbing during apoptosis results from caspase-mediated activation of ROCK I.* Nature Cell Biology 3, 339 – 345.

[47] Pollard, T. D. & Earnshaw, W. C. (2002) *Cell Biology*. Sauders, Elsevier Science (USA), 515-516.

[48] Rychlik, W., Spencer, W.J. & Rhoads, R.E. (1990) *Optimization of the annealing temperature for DNA amplification in vitro*. Nucleic Acids Research, Vol. 18 (21), 6409-6412.

[49] Salto, R., Girón, M. D., Sola, M. M. & Vargas, A. M. (1999) Evolution of pyruvate carboxylase and other biotin containing enzymes in developing rat liver and kidney. *Molecular and Cellular Biochemistry* 200: 111–117.

[50] Promega
http://www.promega.com/guides/pcr_guide/070_22/promega.html (accessed: 18 Aug 2006)

[51] Promega
http://www.promega.com/guides/pcr_guide/070_14/promega.html (accessed: 18 Aug 2006)

[52] NCBI source
http://depts.washington.edu/pceut/pceut_services/DNA-Sequencing-NCBI.pdf#search=%22%20sequencing%20principle%22 (accessed: 19 Aug 2006)

[53] Furuya, H., Yamada, T., Ikezoe, K., Ohyagi, I., Fukumaki, Y. & Fujii, N. (2006) An improved method for Southern DNA and Northern RNA blotting using a Mupid®-2 Mini-Gel, electrophoresis unit. Journal of Biochemical and Biophysical Methods 68, 139–143.

[54] Bustin, S. A. (2000) *Absolute quantification of mRNA using real-time reverse transcription polymerase chain reaction assays*. Journal of Molecular Endocrinology 25, 169–193.

[55] Ekenberg, S. & Hudson, G. (1994) *RNase Protection Assay System: A Versatile Technique for the Analysis of RNA.* Promega Notes Magazine Number 46, 14-17.

[56] L. Overbergh, A. Giulietti, D. Valckx, B. Decallonne, R. Bouillon & C. Mathieu (2003) The Use of Real-Time Reverse Transcriptase PCR for the Quantification of Cytokine Gene Expression. Journal of Biomolecular Techniques 14, 33-43.

Appendix A – Solutions

Waste beaker solution

A 2% (w/v) waste solution was prepared in a beaker by adding 2g of Virkon (Antec, Sudbury, UK) per 100 ml of tap water.

Tris-acetate-EDTA (TEA) buffer solution

In order to prepare the TEA buffer used during the electrophoresis technique 36.5 g of EDTA, 605 g of Tris base, 125 ml of glacial acetic acid were and 2.5 L of RO water mixed. (All the compounds from Sigma, Steinheim, Germany)